Università degli Studi di Padova

Scuola di ingegneria

Corso di Laurea in Ingegneria delle Telecomunicazioni

Performance evaluation of DVB-S2X over satellite channels

Laureando

Giacomo Da Broi

Relatore

Prof. Tomaso Erseghe

Co-relatore

Dr. Stefano Cioni

Anno Accademico 2014/2015

Ai miei genitori che mi hanno sempre sostenuto,
e a Carolina che mi è stata sempre vicina.

We don't get to choose how we start in this life.
Real greatness is what you do with the hand you're dealt.

V.S.

Abstract

A causa della diffusione di nuovi *standard* come HDTV, 3DTV e UHDTV, e alla richiesta di un sempre maggiore *data rate* per sistemi satellitari, è stata introdotta l'estensione di DVB-S2: DVB-S2X. Questo *standard*, grazie all'introduzione di nuovi MODCOD e nuove tecnologie, permette di raggiungere valori più alti di *bit rate* e di disporre di una comunicazione più affidabile.

In questa tesi presenteremo le linee guida di DVB-S2X, come le modulazioni, i codici e l'*interleaver* usati. In seguito approfondiremo le componenti dell'ambiente satellitare, come il TWTA, l'IMUX e l'OMUX, e analizzeremo gli effetti applicati sulle costellazioni. Infine studieremo tre modelli di canale satellitare, che sono *Direct to Home* (DTH), *Very Small Aperture Terminal* (VSAT) e *Digital Satellite News Gathering* (DSNG). Valuteremo la probabilità d'errore sul pacchetto in funzione di P_{SAT}/N_0, e l'efficienza spettrale dei *MODCODs*, confrontando due differenti valori di roll-off: 20% e 5%.

Due to the spreading of new television standards like HDTV, 3DTV and UHDTV, and to the request of higher data rates for satellite systems, the extension of DVB-S2, DVB-S2X, has been introduced. This standard thanks to the introduction of new MODCODs and new technologies permits to reach much higher bit-rate and to have a more reliable communication.

In this thesis we are going to present the general guidelines of DVB-S2X standard, like modulations, coding and interleaving techniques that are used. Afterward we will go through a presentation of all the impairments that can be found in a satellite channel environment, like the characteristic of the traveling wave tube amplifier (TWTA), the phase noise, or the Input Multiplexing (IMUX) and Output Multiplexing (OMUX) filters response, and we will examine their effect on the transmitted constellations. Finally we will study three models of satellite channel which are Direct to Home (DTH), Very Small Aperture Terminal (VSAT) and Digital Satellite News Gathering (DSNG). We will evaluate the Packet Error Rate (PER) versus the P_{SAT}/N_0, and the spectral efficiency of every different MODCOD, comparing two different values of roll-off which are 20% and 5%.

Contents

List of Figures

List of Tables

Chapter 1

Introduction

The evolution of satellite communications began in the late 1950s with the launch of Sputnik, the first artificial satellite. Researches in this field were developed with huge hastiness in those years due to the Cold War, indeed, after the first launch by U.S.S.R., U.S. focused its efforts on any kind of space related technology in order to recover from the Russian launch impact.

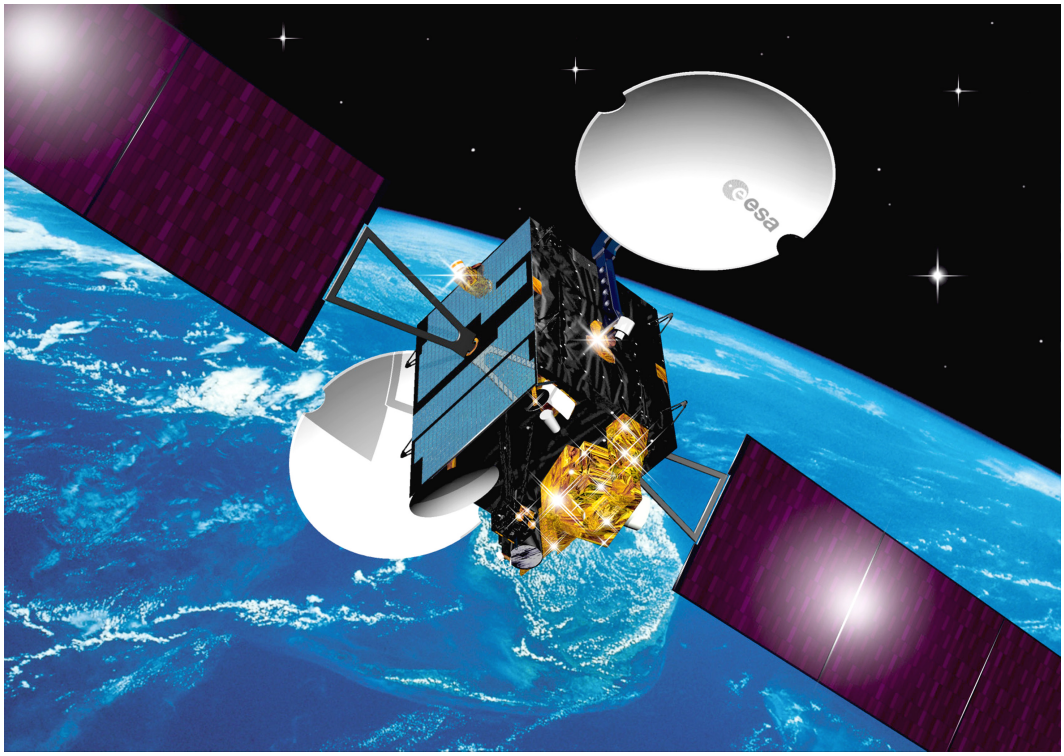

Figure 1.1: ESA Artemis

Satellite communications have some advantages compared to the terrestrial ones, in fact, like is it written in [1], a satellite in a geosynchronous orbit covers almost one third of the Earth's surface, that is much more than a Earth-based transmitter. Hence satellites offer the possibility of covering a large part of the world with voice, TV and data, even areas where is really problematic laying cables and building terrestrial infrastructures, since it is sufficient having an Earth terminal to establish reliable communication.

As stated in [2] the first applications of this new technology were an extension of the terrestrial telecommunication services, like telephone and television. But in the last years, the evolution of the researches in this field, drove to new applications like the creation of satellite systems for domestic television and navigation systems.

In this thesis we will first go through a general presentation of the evolution and the state of the art of satellite communication and digital television, and we will present DVB-S standard. In the second chapter We will present the system architecture of DVB-S2X, and we will explain the most important features for our simulations. Then in chapter three we will describe all the components and the impairments of the satellite channel and finally, in the last chapter, we will present all the channel models used in our study and the results of the simulations.

1.1 DVB project and digital television perspectives

Until roughly 1990, the implementation of a digital broadcast network for television was nearly impossible, this was due to the huge cost of the technology needed in order to accomplish this task. Nevertheless thanks to the evolution of digital technology, the switch from analog to digital became possible, thus it was feasible improving the bandwidth efficiency in the transmissions and the robustness of the communication by mean of FEC (Forward Error Correction).

Digital television provides a huge quality like high-definition video and audio, that is impossible for the old analog one. It gives an higher spectral efficiency as well, since more program channels can be transmitted in the same bandwidth, hence part of the spectrum of analog television can be filled with new contents. Digital television permits new approaches in watching TV like mobile TV, or can interface with other communication systems and computer networks, and finally it permits an interactive experience with the contents.

In digital television systems are present several standardized technologies like source coding, transport stream formats, transmission technology and interactive services. Indeed, since high definition television is in its heyday, it is necessary having an efficient compression technique for video and audio signal, in order to reduce their huge data rate. Hence the goal is finding a good algorithm that reduces the bandwidth and the power required for the transmission of the high-definition signal, without diminishing too much the quality of the service for the users.

In 1988 the MPEG (Moving Pictures Expert Group) was founded, and they standardized several compression algorithms for video and audio compression. The first standard was MPEG-1 used at most for Compact Disks (CD), then it was followed by MPEG-2 and MPEG-4 that are present nowadays in television standards.

In digital television are exploited physical transmission technologies, like modulation and channel coding techniques used is function of the quality of the wireless channel encountered.

From [3] we learn that in 1993 DVB (Digital Video Broadcasting) project was born, with the task of developing TV broadcasting standards for terrestrial, satellite and cable transmissions. The first step in this was designing the first generation standards for television broadcasting: DVB-S for satellite channels, DVB-T for terrestrial TV, and DVB-C for the cable one.

Figure 1.2: Digital video broadcasting

The first generation standards were created with the idea of enable the transmission of High Definition television and Standard Definition television as well. They could also provide the transmission of radio programs and data.

Technically speaking, as can be seen in [4], the three standards have in common an outer encoder and an outer interleaver, then DVB-S and DVB-T have also an inner encoder, since the wireless channel introduces more errors in the transmission. In particular DVB-S as inner encoder uses a 64-state Puncutured Convolutional Code (PCC) with various code rates.

DVB-T, the standard for terrestrial broadcasting, uses the same kind of channel coding technique, and adds an inner interleaver before the bit

mapping in order to suffer less the bursty errors that are more frequent in the terrestrial channel, because time and frequency selectivity are present. Since the terrestrial channel introduces multipath fading and delay spread, this standard makes use of OFDM for the modulation scheme, that works really well in this type of environment.

DVB-C has a simpler implementation because the cable channel is characterized by high SNR and limited bandwidth. Thus are used high order modulations like 16 QAM, 32 QAM, 64 QAM, 128 QAM and 256 QAM.

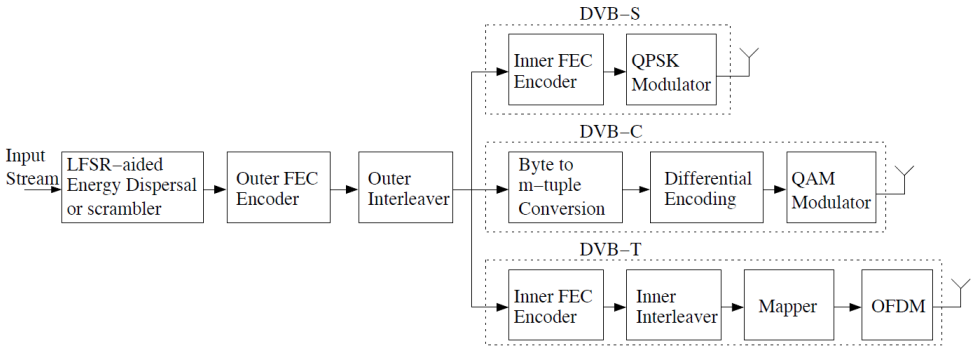

Figure 1.3: First generation standards transmission schemes

However the spread of the HDTV standards and the increasing number of broadcast channels led to the development of the second generation standards like DVB-S2 and DVB-T2 that are more efficient in term of bandwidth and error robustness, since they make use of higher order modulation and improved channel coding schemes like Low Density Parity Check (LDPC) codes.

Like [5] says, nowadays the main trends of the TV service are: an improved quality of the HDTV service, 3DTV service, Ultra High Definition Television (UHDTV) and try to merge TV and web with on-demand and web-assimilated services, so giving a more interactive approach to the user. These progressions are due to the developments in broadcast and coding fields like the improved transmission capacity of DVB-S2 respect to DVB-S, and MPEG-4 source coding.

Since in the coming years the number of 3DTV in the homes is greatly increasing, DVB defined the specification for 3DTV and the commercial requirements as well. 3D technology is based on plano-stereoscopic systems, with two images that must be viewed by left and right eyes nearly in the same time. Beyond the stereoscopic video, another field of research is delivering a free viewpoint television (FTV), so the user can choose the viewpoint of the scene, and watching it from any position in the 3D space. This can be done

using depth maps of the scene.

As far as UHDTV is concerned it is a video format introduced by Nippon Hoso Kyokai (NHK) collaborating with Radiotelevisione Italiana (RAI), European Broadcast Union (EBU) and British Broadcasting Corporation (BBC). The idea is using a broadcasting satellite in 21-Ghz channel, with 600 Mhz of bandwidth, thus it can reach high bit rate level.

However UHDTV can theoretically be provided by DVB-S2 standard, thanks to Adaptive Coding Modulation (ACM) and Variable Coding Modulation (VCM). ACM permits to change the code rate and the modulation in function of the channel conditions, thus, thanks to a feedback channel, it is possible to have information about the quality of the transmission, in order to choose the most efficient modulation and code rate schemes. In order to accomplish this in a broadcast scenario it is necessary dividing the service area in different beams, and control modulation schemes with different feedback channels in favor of the best transmission efficiency.

With this mean it would be possible the UHDTV transmission composing the video signal with two parts: an high priority scheme associated with an highly protected coding scheme and modulation, and a low priority scheme which is much more efficient than other one, that makes use of high order modulation and high code rate. Hence when the channel conditions are good the user can receive the high efficiency signal, so thanks to high rate can watch UHDTV. If the channel conditions are bad the high priority signal is still decodable, as a result of the robust coding and modulation, so the user can receive the TV program as well, even with lower quality.

Finally, talking about satellite interactive TV, nowadays the interaction between the broadcast program and the user is more than changing TV channel, but new services are introduced like video on-demand or voting services, that need technical improvements: for example back-channel availability in order to communicate with network servers, and unicast transmission for the contents request by one user.

1.2 DVB-S2 and its evolution: DVB-S2X

After some years from DVB-S, came out some new issues and possibilities that led to the development of the second generation standard for digital video broadcasting on satellite channels: DVB-S2. These drivers were many: progresses in electronics made possible implementation that were couldn't be done before, so new algorithms and features could be applied; there were new studies about FEC (forward error correction techniques), with really efficient

algorithms that could reach performance near the Shannon limit; there were many requests of services requiring high data rate like HDTV, therefore a more efficient way of transmitting was needed.

QPSK modulation, that was the only one used by DVB-S standard, was a huge restriction regarding the data rate, since there were some Earth stations that could support higher order modulations, thanks to their large antennas. Hence the new standard was designed in a more efficient way, improving the performance of the old one of about 30%.

The new DVB-S2 standard uses several modulations: QPSK, 8PSK, 16APSK and 32 APSK. The choose of APSK constellations instead of QAM is due to their robustness against the distortion given from the high power amplifiers on the satellites thus, even if APSK performance on AWGN channels are worse than QAM performance, in a satellite environment they are preferable.

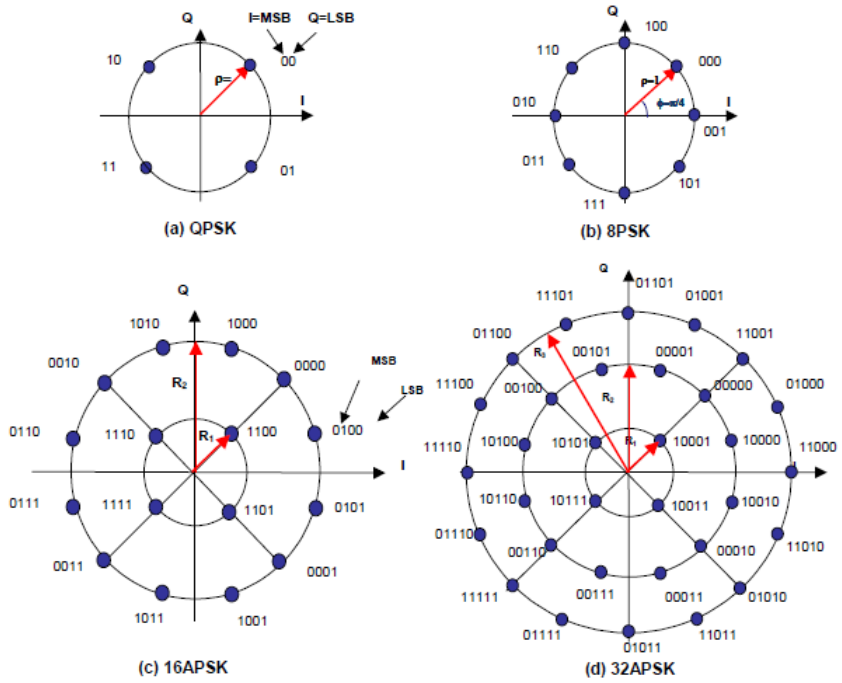

Figure 1.4: Constellations in DVB-S2

As far as channel coding is concerned, LDPC codes were chosen for DVB-S2 standard, and they ensure performance near to the Shannon limit. The available code rates are 1/4, 1/3, 1/2, 3/4, 2/3, 3/4, 4/5, 5/6, 8/9 and 9/10. Two possible frame lengths are also usable: 16200 bit and 64800 bit. The first is really useful when the target is a low-delay transmission, since with

smaller packets there is less delay. The latter is much more robust, it has better performances in term of Packet Error rate (PER). Finally are present a BCH encoder, in order to remove the error floor derived by LDPC undetected errors, and a bit interleaver as well, for improving the code diversity in 8PSK, 16APSK and 32APSK modulations.

One of the main features in this second generation standard is ACM that, like it is described in detail in [6] and [7], permits to menage the use of the transmission resources in function of the channel conditions of a particular user. Indeed we can improve the capacity respect to CCM mode, not wasting efficiency using a rigid physical layer setting that ensures the reliable communication to the worst case conditions system. This component is really useful since in Ku-Band ($12 - 14\,\text{GHz}$) and Ka-Band ($20 - 30\,\text{GHz}$) the atmospheric events, especially rain, are great impairments for the transmission, but these are geographically isolated issues. Thus now the system can adapt an efficient transmission for the zones with clear sky conditions, and a more robust transmission in high fading areas. The idea is making Satellite user Terminals (ST) perform SNIR estimations regularly and report them to the gateway in case of channel variations, hence it can manage the downlink transmission resources and choose the best modulation and coding scheme for every beam. These estimations are performed by mean of pilot symbols. Finally it is possible reaching higher spectral efficiency with a new value of roll off available for the square root raised cosine filter on transmission, that is 0.2 instead of 0.35.

The need to have more resources in order to improve the existent services and to support new technologies, conducted to the development of the extension of 10 years old DVB-S2 standard: DVB-S2X. This new standard will increase the data rate performance, therefore it will possible adding new users in VSAT environments, receiving more TV channels from the broadcasters and it will make possible the diffusion of the new UHDTV, that was feasible with DVB-S2 as well, but with this extension would have a larger impact. DVB-S2X could be employed in different fields like broadcast contributions, IP professional access, disaster recovery and news gathering.

The technologies involved in the standard are several, like it is explained in [8]: for example different values of roll off are used, like 5%, 10% and 15% and advanced filter solutions as well, in order to use the bandwidth in a more efficient manner. Plenty of new MODCODs have been introduced, consequently with ACM it is possible choosing the most efficient modulation and coding setting in every channel condition, in favor of the best performance possible for every coverage zone. This feature along with the addition of higher order modulations like 64-APSK, 128-APSK and 256-APSK can led to an improvement of the efficiency near to 51% with respect to DVB-S2.

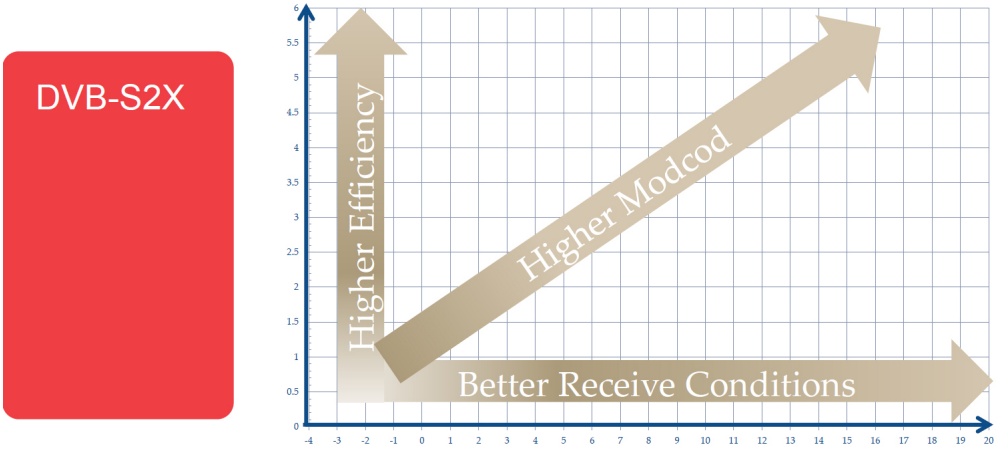

Figure 1.5: Improvements of DVB-S2X

New MODCODs for Very Low Signal-to-Noise Ratio (VLSNR) has been added, for high fading areas and to permit the use of smaller antennas in mobile environments. These new MODCODs can work even at SNR values down to $-10\,\mathrm{dB}$.

DVB-S2X supports also the use of wideband transponders that are now available, with bandwidth values from 70 MHz to hundreds of MHz. This feature permits an higher data rate in the transmission, with gain nearly 20%.

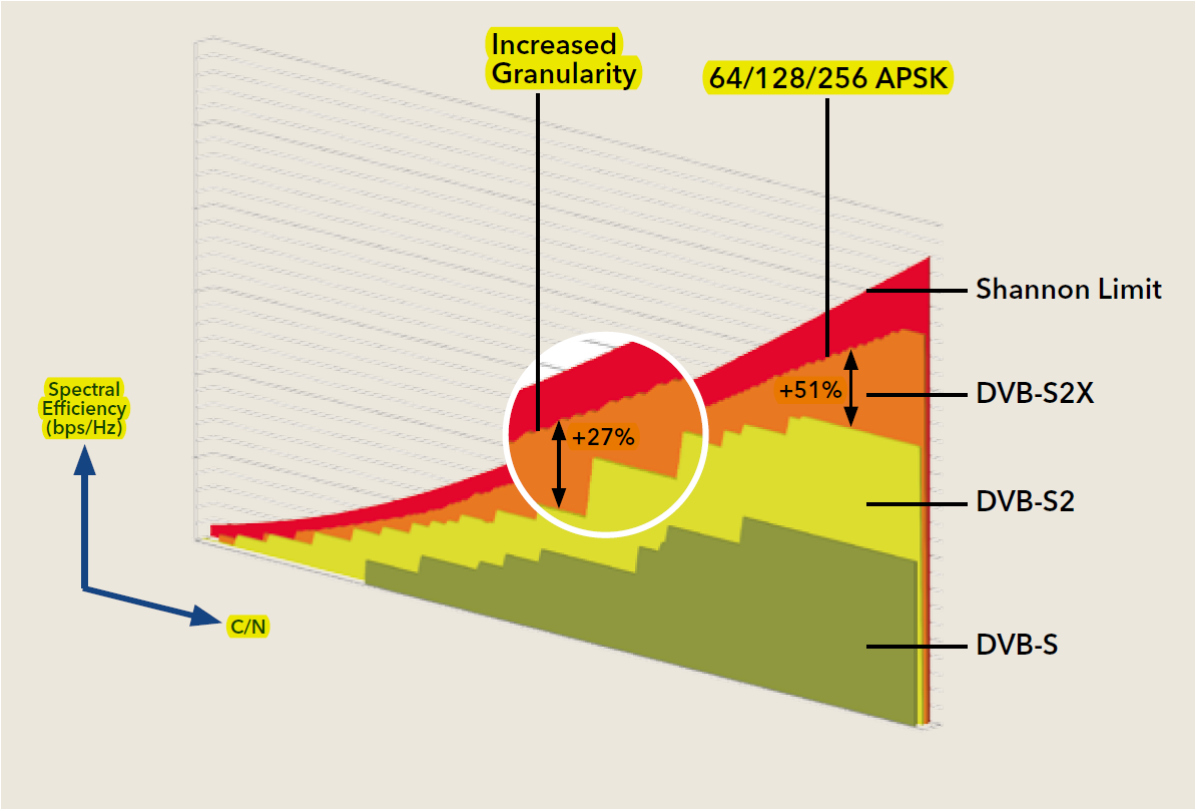

Figure 1.6: Spectral efficiency of DVB-S2X compared to the old standards

Chapter 2

DVB-S2X transmission system

2.1 Transmission scheme

The DVB-S2X architecture is illustrated in Figure 2.1. The scheme, and the description of the system characteristics are accordant to [9], [10] and [11]. The system features are dependent on the application, it should support input stream interfacing, input Synchronization, null-packet deletion, CRC-8 coding, in order to detect errors in a packet-oriented transmission, and, if in presence of multiple streams, it must merge them and finally slicing into data fields.

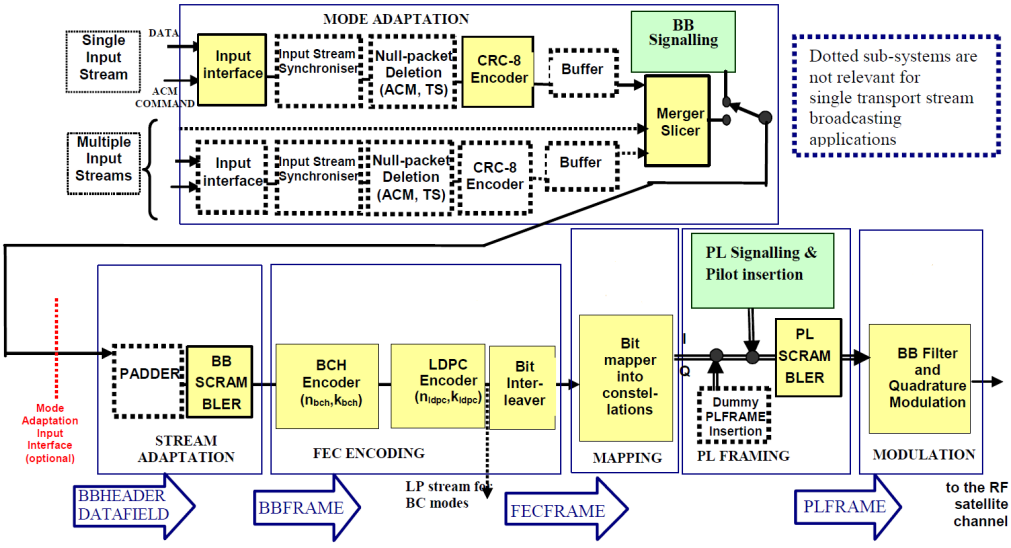

Figure 2.1: DVB-S2X transmission scheme

A signaling information must be added to the data, for communicating

to the receiver which input format and stream adaptation types are used. Finally, in order to complete the Base-Band frame, a stream adaptation sequence is sent, which applies padding to the packets if they don't reach the standard length, and performs scrambling as well.

The Base-Band frame is then processed by the outer BCH encoder and the LDPC inner one. The output codeword, depending on the performance requests, could be $\eta = 64800$ bit or $\eta = 16200$ bit long. The first value is applied for performing better in terms of PER, the latter in order to have lower delay.

Afterward the encoded codeword is mapped to DVB-S2X constellations, which are QPSK, 8PSK, 16APSK, 32APSK, 64APSK, 128APSK and 256APSK. The modulation, and the LDPC code rate as well, is chosen in function of the conditions and of the type of service: for instance QPSK with code rate 1/4 could be used for VL-SNR applications, 8APSK for broadcasting, and 256APSK for various professional services in very good channel conditions, in order to increase Bit Rate.

Finally, for last step before transmission, physical layer signaling must be inserted as well, in order to indicate the MODCOD used, the Start of the Frame (SOF) and other features. In the end the signal is filtered by mean of a Square Root Raised Cosine (SRRC) filter with roll off 5%, 10%, 15%, 20%, 25% and 35%.

2.2 Stream adaptation

DVB-S2X mode adaptation section is not crucial concerning our simulations, therefore our discussion will be focused more on the transmission process, assuming that the Base-Band packet is already built, hence from the stream adaptation.

This section provides to yield to the encoder a constant length and randomized Base-Band frame. The requested length of the Base-Band frame depends from the FEC code rate and, in order to reach the required number of bits, zero padding is applied to fill the frame.

Next step is randomizing the complete Base-Band frame. The polynomial for the Pseudo Random Binary Sequence (PRBS) is:

$$1 + X^{14} + X^{15} \tag{2.1}$$

Figure 2.3 illustrates the scrambling scheme just described.

Since our task is just evaluating the physical layer performance, the packets content is negligible in our simulations, therefore padding and random-

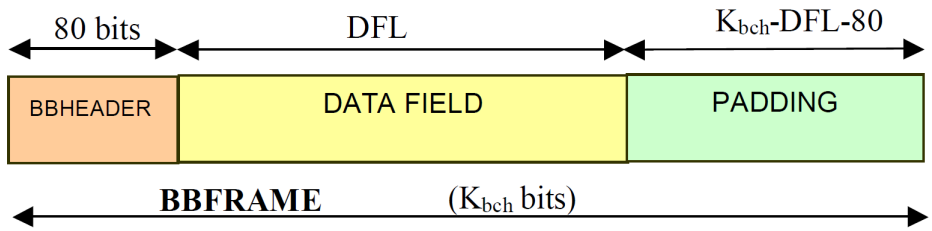

Figure 2.2: BB frame structure

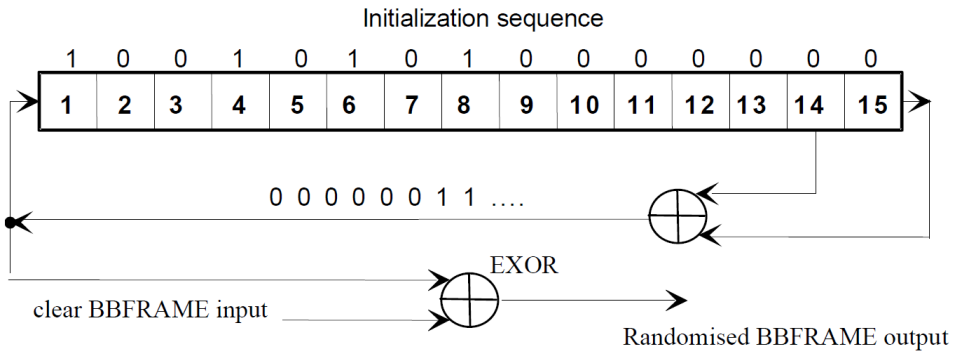

Figure 2.3: BB scrambler structure

ization process are replaced by the generation of PN sequences of the desired length, according to the code rate under test.

2.3 Channel coding

As far as FEC is concerned, the Base-Band Frame is the system input, and FEC Frame the output. The input sequence shall be processed by the outer encoder (BCH), and the inner one (LDPC) in order to compose the final codeword which will be transmitted over the channel. Thus, if we define as BCHFEC the BCH outer encoder parity check bits, and LDPCFEC the inner LDPC encoder ones, the packet will follow the structure shown in Figure 2.4.

As mentioned before, two kinds of packets with different lengths are available: $\eta = 64800$ bit and $\eta = 16200$ bit. The choice between those two is made according to the application and to the performance target of the transmission. An additional type of packet is available as well, and it is $\eta = 32400$ bit long. Its application is over VL-SNR scenarios, and it must be used along with BPSK modulation, coding rate 1/5, 11/45 and 1/3, and requires puncturing. However this kind of transmission will not be taken in consideration

in our study.

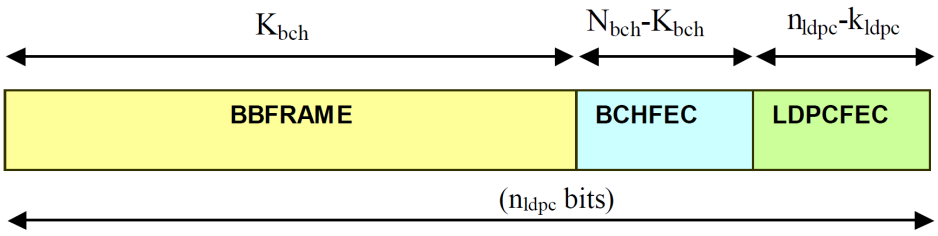

Figure 2.4: FEC Packet structure

2.3.1 BCH encoding

BCH encoder is applied on the Base-Band frame, which is the stream adaptation output. Its task is creating an error protected packet thanks to the BCH code.

In order to build the polynomial of the t-error correcting code, the first t polynomials in the following tables must be multiplied. The number of multipliers changes with respect to the packet length of the final physical layer frame, that could be respectively $\eta = 64800$ bit, $\eta = 32400$ bit or $\eta = 16200$ bit.

$g_1(x)$	$1+x^2+x^3+x^5+x^{16}$
$g_2(x)$	$1+x+x^4+x^5+x^6+x^8+x^{16}$
$g_3(x)$	$1+x^2+x^3+x^4+x^5+x^7+x^8+x^9+x^{10}+x^{11}+x^{16}$
$g_4(x)$	$1+x^2+x^4+x^6+x^9+x^{11}+x^{12}+x^{14}+x^{16}$
$g_5(x)$	$1+x+x^2+x^3+x^5+x^8+x^9+x^{10}+x^{11}+x^{12}+x^{16}$
$g_6(x)$	$1+x^2+x^4+x^5+x^7+x^8+x^9+x^{10}+x^{12}+x^{13}+x^{14}+x^{15}+x^{16}$
$g_7(x)$	$1+x^2+x^5+x^6+x^8+x^9+x^{10}+x^{11}+x^{13}+x^{15}+x^{16}$
$g_8(x)$	$1+x+x^2+x^5+x^6+x^8+x^9+x^{12}+x^{13}+x^{14}+x^{16}$
$g_9(x)$	$1+x^5+x^7+x^9+x^{10}+x^{11}+x^{16}$
$g_{10}(x)$	$1+x+x^2+x^5+x^7+x^8+x^{10}+x^{12}+x^{13}+x^{14}+x^{16}$
$g_{11}(x)$	$1+x^2+x^3+x^5+x^9+x^{11}+x^{12}+x^{13}+x^{16}$
$g_{12}(x)$	$1+x+x^5+x^6+x^7+x^9+x^{11}+x^{12}+x^{16}$

Figure 2.5: BCH polynomials for long packets $\eta = 64800$ bit

$g_1(x)$	$1+x+x^3+x^5+x^{14}$
$g_2(x)$	$1+x^6+x^8+x^{11}+x^{14}$
$g_3(x)$	$1+x+x^2+x^6+x^9+x^{10}+x^{14}$
$g_4(x)$	$1+x^4+x^7+x^8+x^{10}+x^{12}+x^{14}$
$g_5(x)$	$1+x^2+x^4+x^6+x^8+x^9+x^{11}+x^{13}+x^{14}$
$g_6(x)$	$1+x^3+x^7+x^8+x^9+x^{13}+x^{14}$
$g_7(x)$	$1+x^2+x^5+x^6+x^7+x^{10}+x^{11}+x^{13}+x^{14}$
$g_8(x)$	$1+x^5+x^8+x^9+x^{10}+x^{11}+x^{14}$
$g_9(x)$	$1+x+x^2+x^3+x^9+x^{10}+x^{14}$
$g_{10}(x)$	$1+x^3+x^6+x^9+x^{11}+x^{12}+x^{14}$
$g_{11}(x)$	$1+x^4+x^{11}+x^{12}+x^{14}$
$g_{12}(x)$	$1+x+x^2+x^3+x^5+x^6+x^7+x^8+x^{10}+x^{13}+x^{14}$

Figure 2.6: BCH polynomials for short packets $\eta = 16200$ bit

$g_1(x)$	$1+x^2+x^3+x^5+x^{15}$
$g_2(x)$	$1+x+x^4+x^7+x^{10}+x^{11}+x^{15}$
$g_3(x)$	$1+x^2+x^4+x^6+x^8+x^{10}+x^{12}+x^{13}+x^{15}$
$g_4(x)$	$1+x^2+x^3+x^5+x^6+x^8+x^{10}+x^{11}+x^{15}$
$g_5(x)$	$1+x+x^2+x^4+x^6+x^7+x^{10}+x^{12}+x^{15}$
$g_6(x)$	$1+x^4+x^6+x^7+x^{12}+x^{13}+x^{15}$
$g_7(x)$	$1+x^2+x^4+x^5+x^7+x^{11}+x^{12}+x^{14}+x^{15}$
$g_8(x)$	$1+x^2+x^4+x^6+x^8+x^9+x^{11}+x^{14}+x^{15}$
$g_9(x)$	$1+x+x^2+x^4+x^5+x^7+x^9+x^{11}+x^{12}+x^{13}+x^{15}$
$g_{10}(x)$	$1+x+x^2+x^3+x^4+x^7+x^{10}+x^{11}+x^{12}+x^{13}+x^{15}$
$g_{11}(x)$	$1+x+x^2+x^4+x^9+x^{11}+x^{15}$
$g_{12}(x)$	$1+x^2+x^4+x^8+x^{10}+x^{11}+x^{13}+x^{14}+x^{15}$

Figure 2.7: BCH polynomials for medium packets $\eta = 32400$ bit

The encoding procedure of a Base-Band frame $m = (m_{k_{bch}-1}, m_{k_{bch}-2}, ..., m_1, m_0)$ is the following:

- Perform the product between $x^{n_{bch}-k_{bch}}$ and the message polynomial $m(x) = m_{k_{bch}-1}x^{k_{bch}-1} + m_{k_{bch}-2}x^{k_{bch}-2} + ... + m_1x + m_0$;
- Divide the result of the multiplication by the generator polynomial of the code $g(x)$ found from the previous tables, and save the remainder $d(x) = d_{n_{bch}-kbch-1}x^{n_{bch}-kbch-1} + ... + d_1x + d_0$;
- The resulting codeword, output of the BCH encoder, will be $c(x) = x^{n_{bch}-k_{bch}}m(x) + d(x)$.

2.3.2 LDPC encoding

In DVB-S2X LDPC systematic encoding is applied, whose input is an information frame k_{lpdc} long, which is encoded in a codeword of size η_{lpdc}.

These kinds of codes are defined by sparse parity check matrices H and specifically, in DVB-S2X, in order to reduce the complexity, the matrix is in the form

$$H_{(N-K)\times N} = \left[A_{(N-K)\times K} B_{K\times N}\right]$$

where B is a staircase lower triangular. A periodicity of $M = 360$ has been set to limit the storage, as explained in [12] as well.

The goal of the encoder is to find $\eta_{ldpc} - k_{ldpc}$ parity bits, and to append them to the input frame. The procedure is briefly explained here:

- inizialize to zero all the parity check bits;
- accumulate the first bit of the frame which has to be encoded in the position specified in the table in [9];
- do this operation for the following 359 bit as well, but the accumulation position must be set according to $(x + m \bmod 360 \times q) \bmod (\eta_{ldpc} - k_{ldpc})$. Where q is a parameter which is predefined in function of the code rate;
- apply the same procedure periodically (with period equals to 360);
- finally, starting with $k = 1$, perform

$$p_k = p_k + p_{k-1} \tag{2.2}$$

  all these sums are achieved in the Galois field.

2.3.3 Bit interleaver

Bit interleaving is applied to all modulations but BPSK and QPSK. The input is LDPC-coded packet, which is written in the interleaver column-wise. Instead the rows are read in a defined interleaving pattern, which depends on the MODCOD of the transmission. These reading patterns can be easily found in [9].

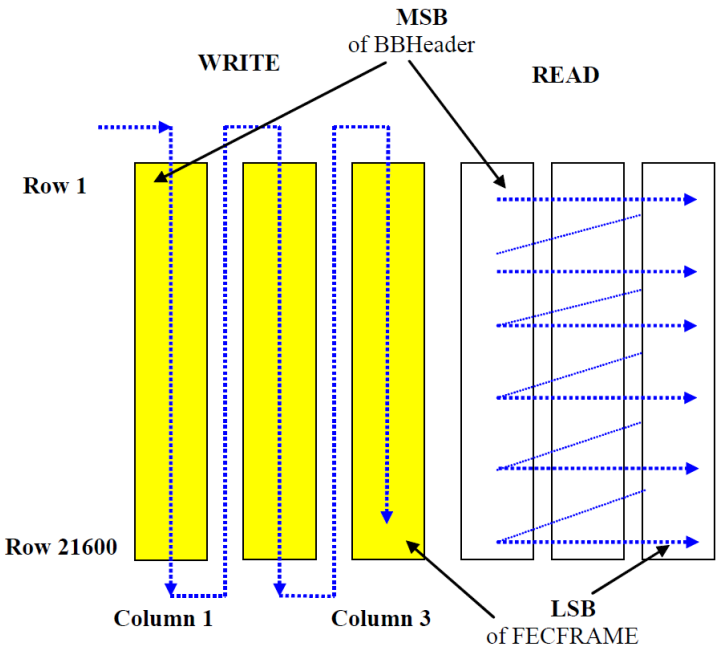

Figure 2.8: Example of bit interleaving for 8PSK

2.4 Mapping into constellations

BPSK $\frac{\pi}{2}$ modulation is the lowest order modulation available, and it is used specifically in VL-SNR scenarios, because of its robustness. Then classic QPSK and 8PSK modulation are used, with Gray coding and normalized energy per symbol $\rho = 1$. Besides a new modulation has been introduced in DVB-S2X, which is 8 APSK (Figure 2.9).

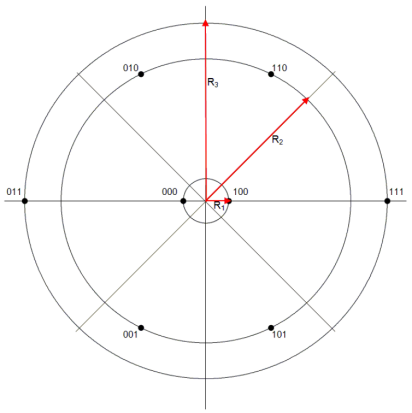

Figure 2.9: Example of 2+4+2APSK constellation

The constellation points are disposed on three rings, two points in the first ring, four points in the second, and the last twos in the third. The radii of the circles are optimized with respect to AWGN channel, and to coding rate.

Then two types of 16APSK modulations are available: 4+12APSK, thus with 4 constellation points in the inner ring and 12 in the outer one, and 8+8APSK (Figure 2.10) that has 8 points on both circles. Also in these kinds of modulations the radii of the rings are optimized in function of the code rate and the packet length.

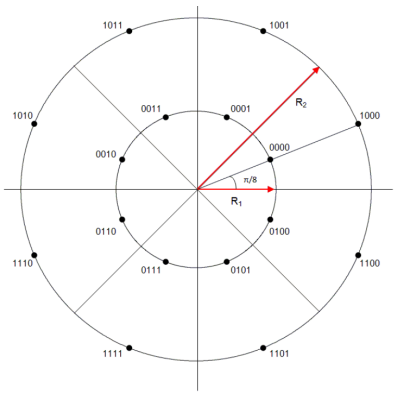

Figure 2.10: Example of 8+8APSK constellation

In 32APSK case, it is still available from DVB-S2 the old 4+12+16APSK constellation. But a four-rings constellation has been introduced as well, which has four points in the first circle, eight in the second, then four in the third and finally sixteen in the most external ring. This constellation is illustrated in Figure 2.11.

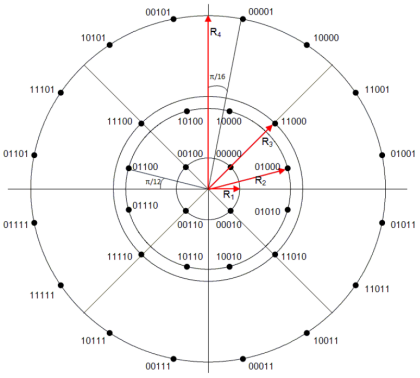

Figure 2.11: Example of 4+8+4+16APSK constellation

For higher order modulations DVB-S2X introduced 64APSK, 128APSK and 256APSK. Three kinds of 64APSK constellations are available: 16+16 +16+16APSK four rings with the same amount of points in every circle, 8+16+20+20APSK and finally, with four rings as well, 4+12+20+28APSK (Figure 2.12).

Figure 2.12: Example of 4+12+20+28APSK constellation

Finally the three highest order modulations available in the standard are 128APSK, and two versions of 256APSK. The exact values of the points are specified in [9], here we show some examples of the constellation shapes in Figures 2.13 and 2.14.

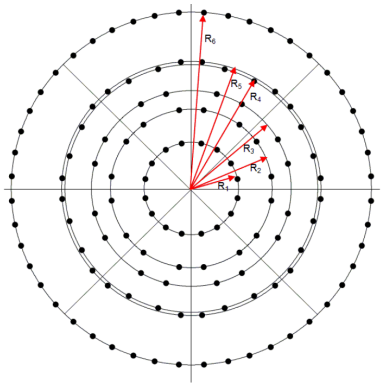

Figure 2.13: Example of 128APSKconstellation

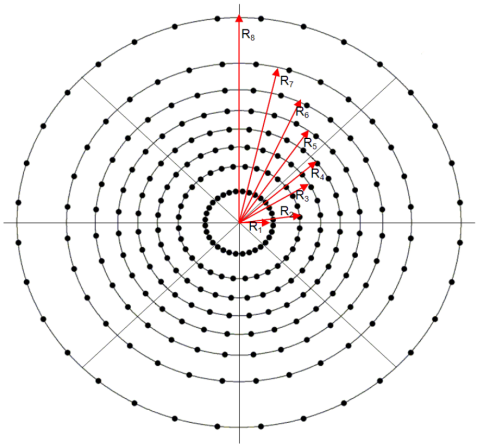

Figure 2.14: Example of 256APSK constellation

2.5 SRRC Filters

In order to accomplish the signal transmission, we need a square root raised cosine filter. We remind the function of this one, which is given by:

$$H(f) = \begin{cases} 1, & for\,|f| < f_N(1-\alpha) \\ \left[\frac{1}{2} + \frac{1}{2}\sin\frac{\pi}{2f_N}\left(\frac{f_N - |f|}{\alpha}\right)\right]^{\frac{1}{2}}, & for f_N(1-\alpha) \\ 0, & otherwise \end{cases} \tag{2.3}$$

in this equation f_N indicates the Nyquist frequency and α the roll-off of the raised cosine. The pulses are shown in figure 2.15, taken from [13].

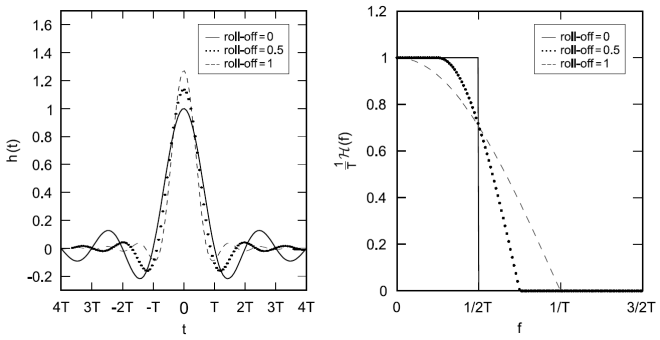

Figure 2.15: Square root raised cosine pulse

In DVB-S2X several roll-off values are available: 35%, 20%, 15%, 10% and 5%. In in this thesis we will focus our simulations on two kinds of roll-off

factors, that are 20% and 5%. Finally, in order to build the modulated signal that will be sent over the channel, it is necessary multiplying the in-phase and in-quadrature parts by $\sin(2\pi ft)$ and $\cos(2\pi ft)$, where f is the system carrier frequency. Then it is sufficient summing the two products, and send the signal in the RF channel.

Chapter 3

Satellite channel impairments

DVB-S2x performance must be evaluated in a satellite environment, since AWGN channel performance are not indicative for what concerns our tasks. In satellite channels there are some impairments that affect with linear and non-linear distortion the modulated signal, attenuation and phase noise, which must be taken into account in the simulations in order to have precise and realistic system performance.

The basic channel model, where all the impairments that we are going to examine are found, is the one presented in [14], and shown in Figure 3.1. Even though it is only a basic model, it is really useful for our purposes to analyze all the components of a satellite communication scheme.

The performance in this kind of channel greatly differs from the AWNG one. This is due to the accumulation of non-linear and linear distortions and phase noise at the receiver, which can lead to a really consistent performance degradation. This especially happens using high order modulations, which are greatly affected by distortion and phase noise phenomena. Fortunately by mean of pilot-aided (PA) schemes and pre-distortion techniques, it will be possible counteracting these impairments.

The first system block is FEC encoder, whose outputs are the transmitted codewords. Like it has been explained in Chapter 2, the transmission chain continues with the mapping on the constellations, but in this case, before the SRRC filter, it is possible to apply an optional digital pre-distortion, in order to diminish the non-linear channel effects. After the transmission filter an high-power amplifier (HPA) is placed, but this will be not a great impairment for the performance, since it is usually working with a huge value of back-off, therefore in the linear region. This assumption is possible because in earth stations power is not usually a issue. After these considerations the Earth's station HPA will be neglected in the simulations.

There is an AWGN contribution on the uplink, but it is considered neg-

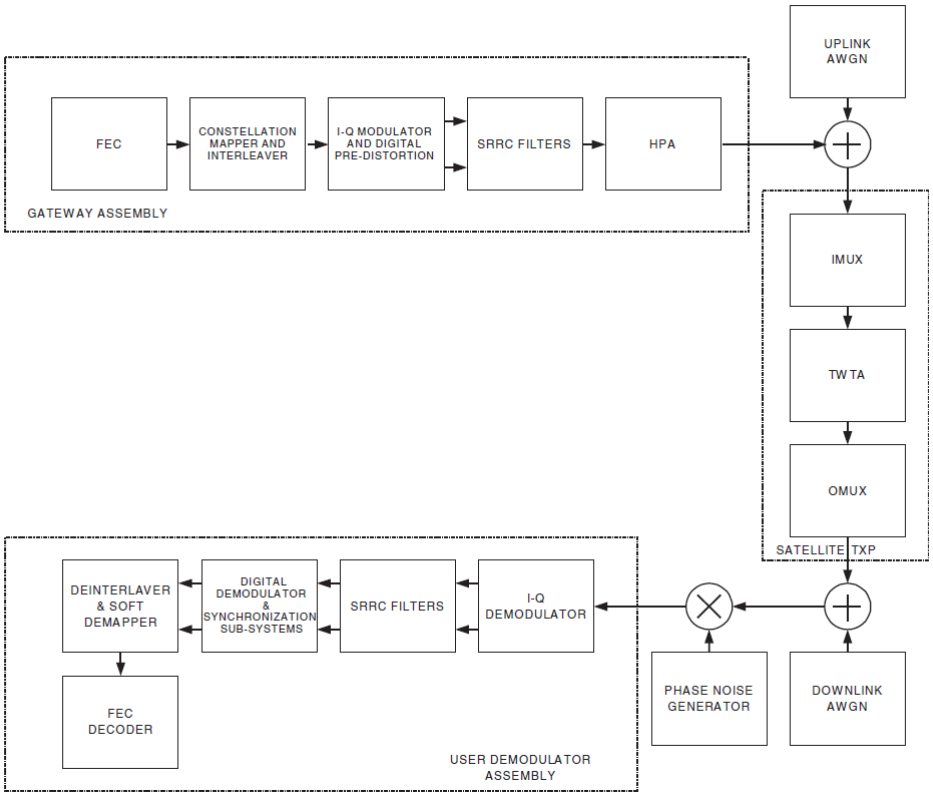

Figure 3.1: Basic satellite channel scheme

ligible. The transponder is placed on the satellite payload, and it is the most important and problematic part. It is composed of three elements: two filters, IMUX and OMUX, which select the channel in use, but introduce inter-symbol interference, and Traveling Wave Tube Amplifier (TWTA) that is an HPA which amplifies the carrier, but introduces non-linear distortion. The latter cannot be neglected in the analysis, because on the satellite segment power is a huge issue, unlike in Earth stations, hence it is preferable working in a point near to saturation, in order to have the best power efficiency. On downlink there are AWGN and attenuation due to atmospheric phenomena, which are enclosed in the AWGN block in Figure 3.1. And finally, before the demodulator, phase noise must be applied to the signal, due to the low noise block (LNB). Then the receiver scheme is composed by the matched filter, demodulation and synchronization systems, deinterleaver and soft demapper, and finally the FEC decoder, for recovering the transmitted bits.

In the following Chapter we will go through an in-depth analysis of the

most important and relevant components of the satellite channel, in order to understand better the channel models simulated in Chapter 4.

3.1 Transponder

The satellite transponder, which is the equipment that allows the correct reception, the amplification, and the transmission of the radio signal, is composed by three principal parts: IMUX and OMUX filter, and the TWTA.

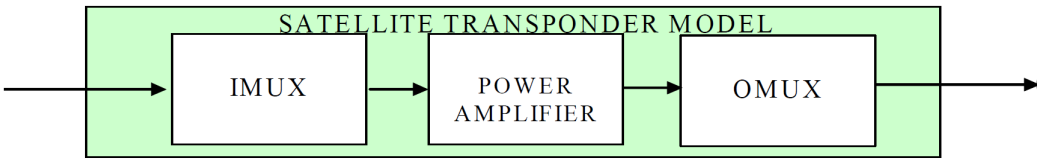

Figure 3.2: General transponder scheme

3.1.1 IMUX and OMUX filters

The purpose of these filters is dividing the different transmission channels. This is necessary because when a signal is amplified by an HPA along with other carriers, or interferences due by adjacent channels, there will be an intermodulation noise generation. Thus this procedure, called channelization, it is always advisable. Even in multi-carrier scenario, it is possible to limit interferences due to other satellites, or other beams.

Input multiplexer (IMUX) is a band-pass filter which is located in the first part of the transponder, and selects the bandwidth correspondent to the carrier that has to be amplified.

Output multiplexer (OMUX) is a band-pass filter as well, but as it can be seen in Figure 3.2, is placed at the end of the transponder chain. Its function is to recombine the channels after the amplification by the HPA.

The Amplitude response, and the Group Delay models of IMUX and OMUX which are applied in this thesis are the one that are suggested by [15], and their group delay and frequency response are shown in Figures 3.3 and 3.4.

These models are designed for transponder bandwidth of 36 MHz, and a carrier spacing between different channels of 40 MHz. But in [9] is suggested a formula for scaling the responses even for larger transponder bandwidth. The

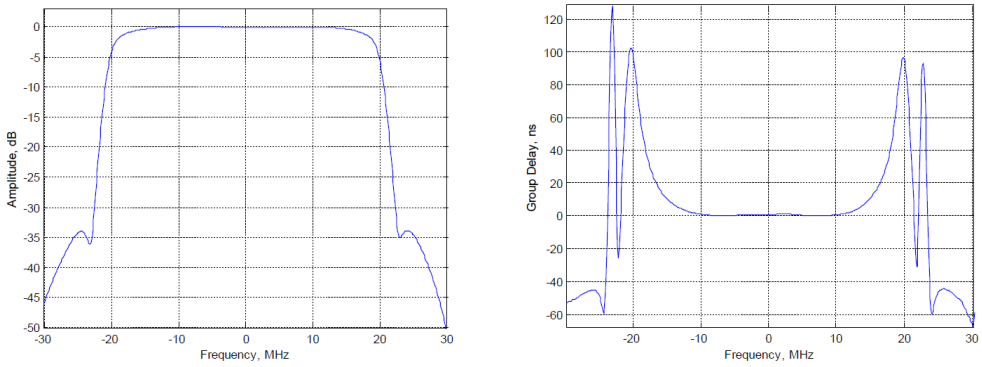

Figure 3.3: IMUX Amplitude response and Group Delay response

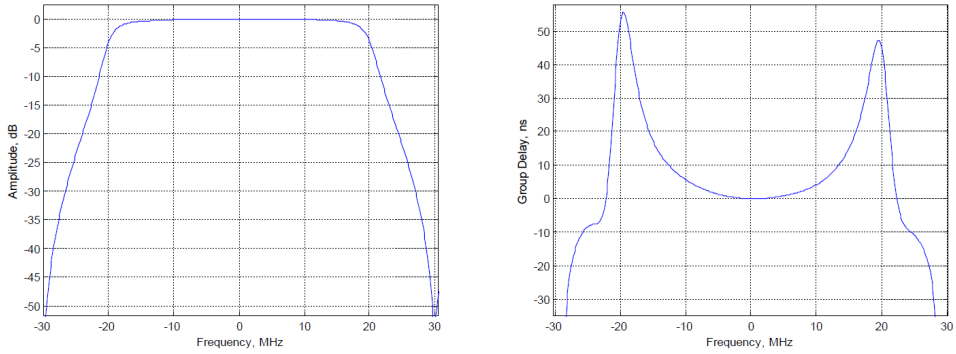

Figure 3.4: OMUX Amplitude response and Group Delay response

aforementioned relations for Amplitude and Group Delay are the following

$$A\left(f\right) = A\left[f\frac{B}{36}\right] \tag{3.1}$$

where A is the amplitude of the frequency response and B the bandwidth. The scaling formula for the Group Delay is

$$G(f) = \left(\frac{36}{B}\right) G\left(f\frac{B}{36}\right) \tag{3.2}$$

where G is the Group Delay, and the other parameters are analogous to the previous expression.

These two relations do not perform the exact response for any bandwidth, but they are good approximations for our tasks.

There are two important parameters that define these filters, which are: nominal transponder bandwidth, and transponder frequency spacing. The

first is the amount of bandwidth where the frequency response amplitude is almost constant. The latter is the advisable distance between the channels, thus between the center frequencies of every transponder. In the simulations we are going to use transponders with 36 MHz of nominal bandwidth, and 40 MHz of carrier spacing for a certain scenario. And also a 500 MHz transponder with 225 MHz of frequency spacing for a different channel setting.

The aforementioned filters are required in satellite systems, but they introduce linear distortion and Inter-Symbol Interference (ISI) due to their non-linear phase and frequency responses. Consequently, even though they must be used, they cause transmission degradation. This ISI term can be modeled with a Gaussian random variable like it is shown in [14].

3.1.2 TWTA

Traveling Wave Tube Amplifier (TWTA) is the most important component of the satellite channel. It is a non-linear HPA, thus it introduces non-linear distortion on the constellations sent by the transmitter. This amplifier has to be driven as close to saturation as possible, because energy is precious in satellite environment, therefore it is mandatory to reach the most efficient working point for every case. This is always feasible when low-order modulations are employed, but with high-order modulations like 32-64-128-256APSK distortion becomes very consistent, and the transmission will be affected by huge performance degradations.

The key parameters, as far as TWTA is concerned, are Input Back-Off (IBO) and Output Back-Off (OBO), and their relation is represented by the AM/AM and AM/PM characteristics. In order to avoid distortion in high-order modulations, TWTA input signal is processed on purpose in a lower power level, thus the working point of the HPA is shifted in the linear region. The power amount that transfers the amplifier working point is called IBO, and the correspondent output power loss is called OBO. These twos are really important parameters, and they have to be carefully chosen in order to simulate end-to-end system performance. In fact in DVB-S2X there are some modulations which do not work in saturation mode, even in no-noise scenario.

In Figure 3.5 are shown AM/AM and PM/PM characteristics of a non-linearized TWTA, which is going to be used in the simulations. It can be noticed that the working point is supposed to be at $IBO = 0\,\text{dB}$, which corresponds of course at $OBO = 0\,\text{dB}$, since the input power is not diminished. But if the IBO value is changed there is an almost linear relation between input and output power, hence the distortion phenomena are limited. A lin-

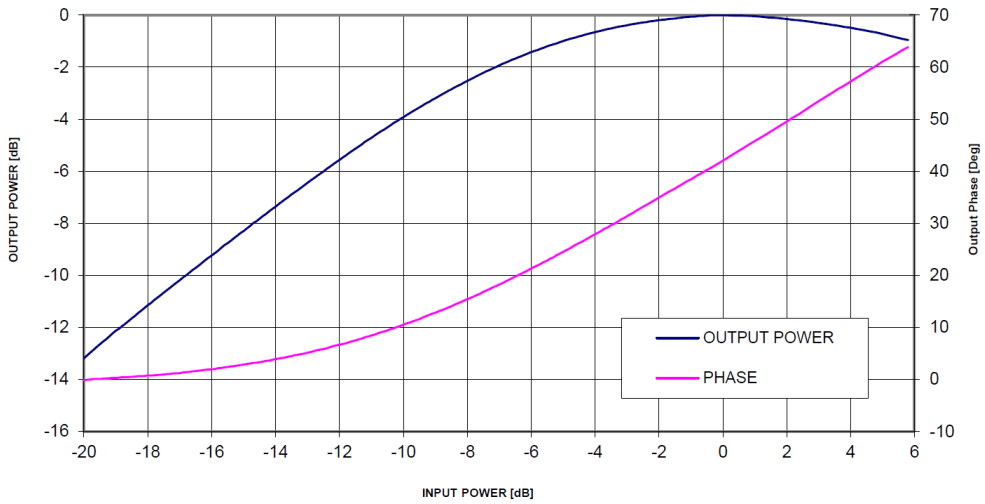

Figure 3.5: TWTA AM/AM and AM/PM characteristics

earized transponder model, whose AM/AM and AM/PM characteristics are shown in Figures 3.6 and 3.7, will be used as well in some scenarios that we are going to simulate.

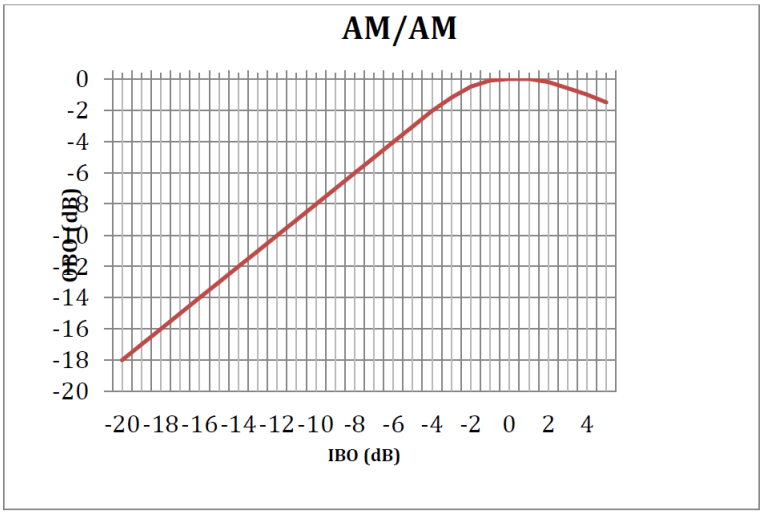

Figure 3.6: TWTA linearized AM/AM characteristics

In Figure 3.8 instead, the effects of the transponder application on the constellations are illustrated. The scatter plots in 3.8, have been performed setting $IBO = 0\,\text{dB}$, thus driving the HPA at full power, and with no noise.

It is clear that it is feasible exploit all HPA power in low-order modulations like 8APSK, because, even if the constellation points are distorted,

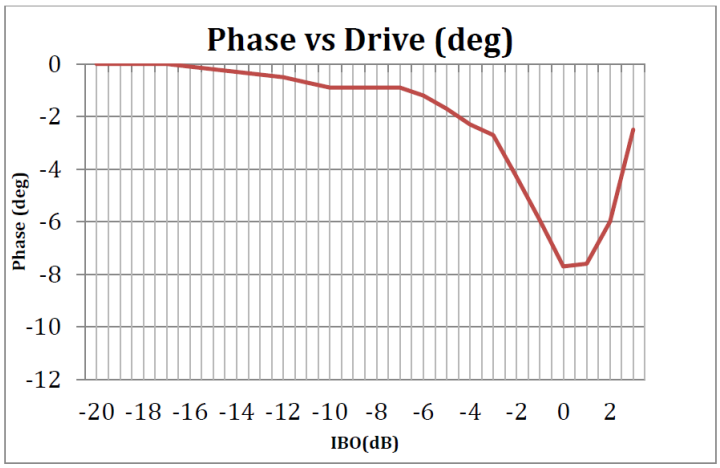

Figure 3.7: TWTA AM/PM characteristics

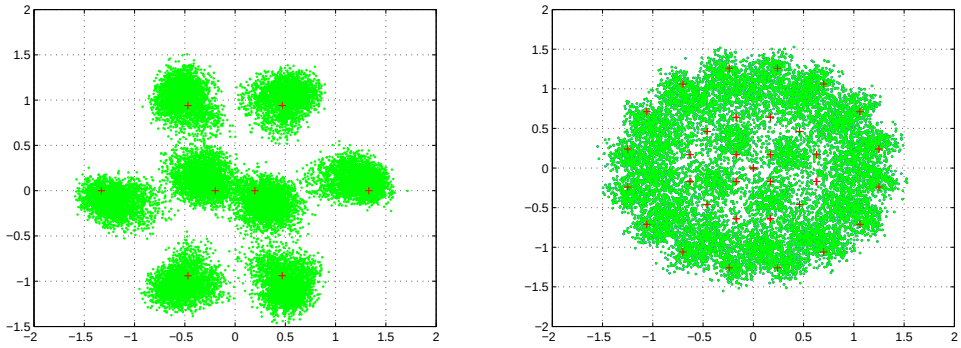

(a) (b)

Figure 3.8: (a) Scatter plot of 8APSK with IBO=0dB, (b) Scatter plot of 32APSK with IBO=0dB

the waveforms are still distinguishable by the decoder. In case of an higher order modulation like 32APSK, despite the efficient power use of the TWTA, performance will get worse with IBO equal to zero, because the constellation is much more distorted, and, if AWGN is taken into account, we get really bad performance. In more efficient modulation scenarios, like 128APSK or 256APSK, with $IBO = 0\,\text{dB}$ is impossible reaching the waterfall region, even with really high (and unrealistic) SNR values.

The scatter plot in Figure 3.9 are referred to the same constellations, but with $IBO = 10\,\text{dB}$ (value that is too high for both transmission settings, but it has been chosen for illustrative manner), hence the HPA is working

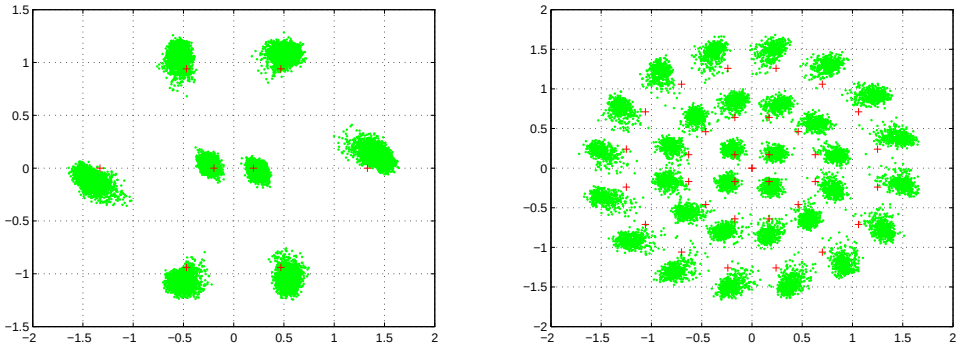

(a) (b)

Figure 3.9: (a) Scatter plot of 8APSK with IBO=10dB, (b) Scatter plot of 32APSK with IBO=10dB

in a strongly linear point. It is possible to notice that constellations in this case are much less distorted, and the points are less spread in the complex plane. The distortion issue is now solved, but the transponder is working in a really inefficient manner, because it is wasting much power. Therefore in every condition, and in every modulation setting there is an optimum trade off between power efficiency and distortion. Further considerations will be examined in Chapter 4, in order to perform the Packet Error Rate (PER) simulations.

After such assumptions we can state that the performance given the channel non-linearity, and the the warping effects of the constellations are well described by the following expression:

$$\left[\frac{E_s}{N_0}\right]_{req}^{NL}[dB] = \left[\frac{E_s}{N_0}\right]_{req}^{AWGN}[dB] + D_{tot}\,[dB] + OBO\,[dB] \tag{3.3}$$

where $D_{tot}\,[dB]$ is the non-linear degradation of the performance, $\left[\frac{E_s}{N_0}\right]_{req}^{NL}[dB]$ is the SNR value needed in order to reach a certain value of PER in the non-linear channel, $\left[\frac{E_s}{N_0}\right]_{req}^{AWGN}[dB]$ is the SNR requested to have the aforementioned performance with the same MODCOD in an AWGN scenario, and finally $OBO\,[dB]$ is the power loss given by the choice of shifting the working point of the HPA from the saturation point.

The degredation can even get worse in another type of scenario, that has to be taken into account as it will be present in the channel models that we are

going to simulate, which is the multicarrier-mode. Like [16] states, since the bandwidth availability is increasing, and thanks to the multi-beam systems, multi-carrier in one single transponder is widely spreading. This application of TWTA can lead to higher performance degradations in term of PER for the introduction of another distortion component along with the previous one, which is the intermodulation (IM) distortion due to the adjacent carriers, that are amplified by the non-linear HPA. Sometimes, especially in case of input power unbalance on the transponder, those degradations can be critical. We will study more in depth this effect in Chapter 4, testing the DSNG channel.

3.2 Channel interference

As presented in a detailed manner in [17], there are various kind of interferences in a satellite system, such as adjacent channel interference, co-channel interference, cross-channel interference and adjacent system interference.

In uplink, thus in the satellite payload input, the possible interferents are Earth Stations (ES) that transmit in the same system, or belonging to others as well. Instead in downlink the ESs input interference is due to satellites of the same system which transmit together, or to totally different systems. Of course the impact of these interferences is diminished thanks to the multiple access schemes, like Frequency Division Multiplexing Access (FDMA), Time Division Multiplexing (TDMA) or the transmission on different polarizations. However in our simulation scenarios these impairments must be considered in some cases.

3.2.1 Adjacent channel interference

This kind of interference is due to elements of the same system. For instance in uplink is caused by ESs belonging to the same system, and transmitting to the same satellite. Instead as far as downlink is concerned the interference comes from the transmission from the satellite to the ESs of the same spot-beam.

As it will be explained in the channel models in Chapter 4, these phenomena are decreased by mean of various medium access techniques, like it was mentioned before.

3.2.2 Co-Channel interference

Co-Channel interference is a kind of interference induced by signals transmitted by ESs of the same system, using the same carrier and polarization of the

carrier under test, but belonging generally to different beams, or to the same as well in Code Division Multiple Access (CDMA) case. If the stations are located in the same beam, and use CDMA technique we are talking about intra-beam interference, otherwise inter-beam interference.

In uplink scenario, where the transmitting ESs create interference between each other, the problem is eased by the antenna pattern, or by the orthogonality provided by CDMA. In the downlink case, the problem is correlated with the antenna roll-off of the adjacent spot beams.

3.2.3 Cross-Channel Interference

Cross-Channel interference is caused by ESs and satellites that are in the same system, using the same carrier frequency, but with an orthogonal polarization with respect to the carrier under test. In both cases of uplink and downlink scenario, this issue is stemmed by mean of cross-polarization isolation of the antennas of the ESs and on the satellites.

3.2.4 Adjacent System Interference

This last type of interference is referred to all the phenomena originated by other communication systems, different from the one to whom the carrier under test belongs. The impairment is generated by signals from the aforementioned systems, using the same polarization and carrier frequency of the useful information signal. In the case of low elevation link, it ought to be taken in account also the interference of some adjacent terrestrial communication systems, but it will not be our case.

3.3 Phase noise

Phase noise (also know as phase jitter) is a disturbance introduced by the non-ideal oscillator at the receiver. Like [13] explains, the signal is received in the following form:

$$r(t) = V_0 [1 + a(t)] \cos\left(\omega_0 t + \varphi_j(t) + \frac{dt^2}{2}\right) \tag{3.4}$$

where $v(t)$ is the received pulse, $a(t)$ is an amplitude impairment and φ_j is the phase noise. Since the amplitude noise can be often neglected, the insertion of the phase noise in a general transmission system can be accomplished like in figure 3.10.

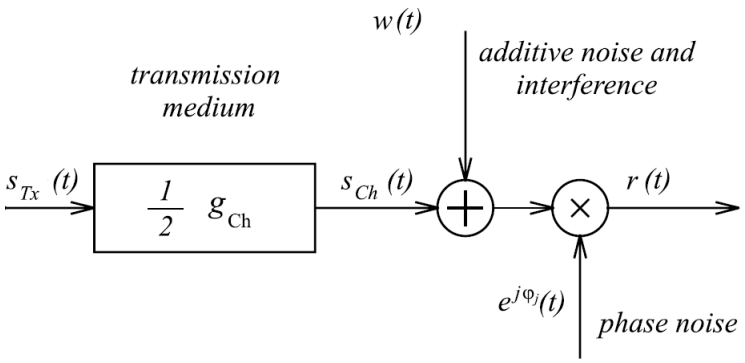

Figure 3.10: Phase noise in a generic transmission system

The phase jitter is a random process, and its Power Spectral Density (PSD) is given by a certain mask which expresses the values of the PSD in dBc, which are dB carrier namely the power given by this noise divided by the power of the carrier under test.

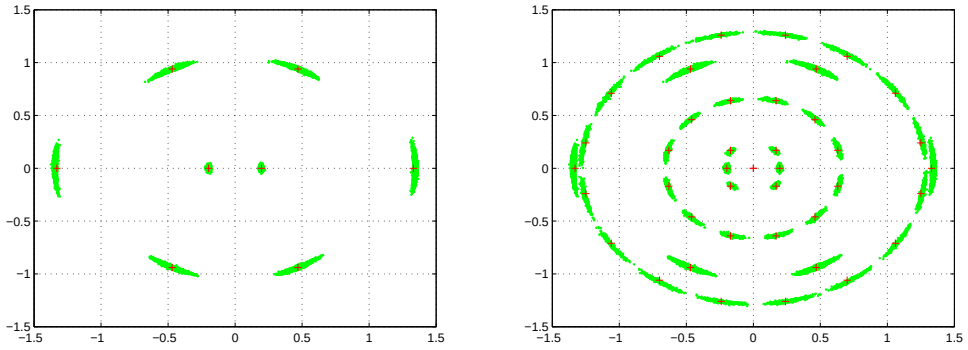

(a) (b)

Figure 3.11: (a) Scatter plot of 8APSK affected by phase noise, (b) Scatter plot of 32APSK affected by phase noise

In this thesis, for the simulations, different phase noise masks will be used for every different scenario. The choice of every simulation mask is given by the channel models defined in [15]. However we will go more in depth concerning this topic in Chapter 4, where the complete channel model will be described.

Finally, in order to have a general idea of the phase noise effect on the transmission, it is possible to examine it on the constellations. In the previ-

ous considered examples (8APSK and 32APSK), phase noise creates on the received points the outcome that can in be seen in Figure 3.11. The diagrams are plotted applying only the phase noise impairment, taking into account no channel.

3.4 Amplitude distortion

Finally one last distortion type is taken into account, which is the one generated by the coaxial cable used in the system. This impairment introduces some frequency selective distortion in the amplitude of the signal, thus the LNB is designed with a frequency response that can balance the cable impairment. The relevance of the amplitude distortion depends from many factors, like the length and the quality of the cable, and the model of the LNB.

However in the simulations performed in this thesis it will be taken into account a variation of $\pm 2\,\text{dB}$ over 500 MHz band.

In Figure 3.12 is shown the cable impairment scheme, where Δ is a sine wave with 1.5 dB amplitude and period $T = 50\,\text{MHz}$.

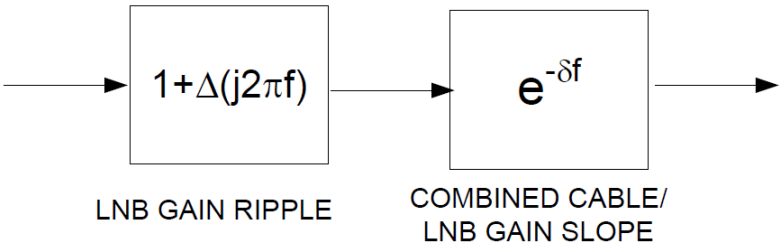

Figure 3.12: Amplitude distortion scheme

3.5 Overall effect of the impairments on transmission

Thanks to computer simulations performed in [18], it is possible having an idea on how much degradation the satellite channel impairments introduce.

These simulations are operated using a 36 MHz transponder, varying the transmission baud rate and the roll-off of the SRRC filter, in order to understand how the performance of the system change in function of these parameters.

The first situation examined is the degradation given by the ISI generated by the non linear phase of IMUX and OMUX filters. Figure 3.13 explains that with higher symbol rate the Carrier on interference ratio ($\frac{C}{I}$) gets worse. But also the choice of the roll-off factor is relevant, since from a side the spectrum sidelobes due to the truncation of the transmitting filter have higher values using lower roll-off, from the other hand an higher roll-off increases interference, because of the larger spectrum of the signals, whose the tails are distorted by the filters.

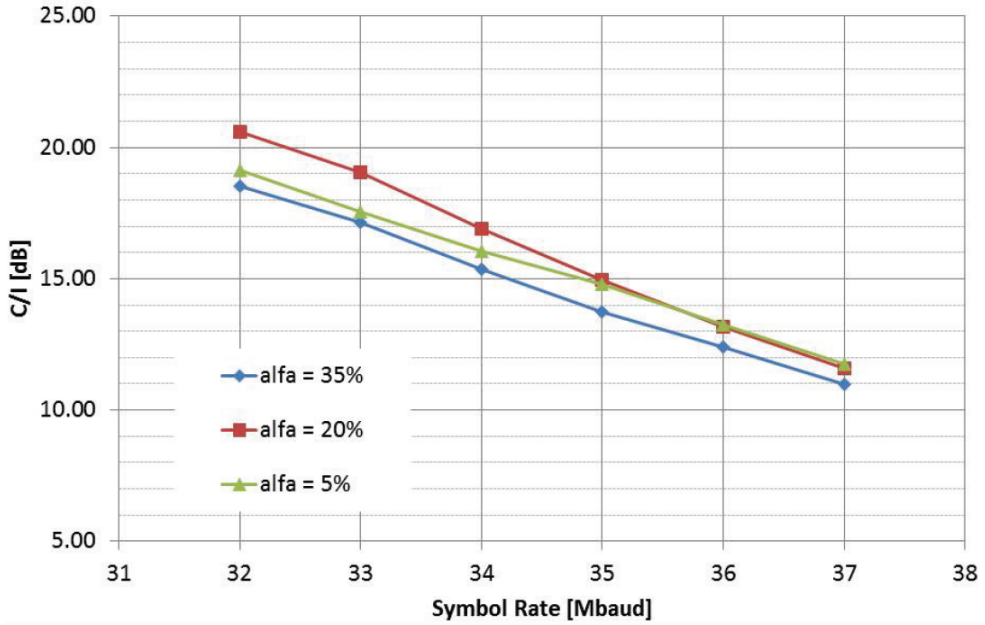

Figure 3.13: $\frac{C}{I}$ due only to the ISI

In the following simulation, performed in [18] as well, the slope of $\frac{C}{I}$ versus the symbol rate is evaluated taking into account the non-linear effect of the HPA on board, some uplink and downlink interferences and the ISI introduced by the filters as well. The modulations used are QPSK and 16APSK. The results are shown in Figure 3.14, and it can be noticed that the channel non linearity effect affects more higher order modulations than lower order. As a matter of fact 16APSK seems to be much more distorted by the non-linearity, as we expected.

Finally, in Figure 3.15, is illustrated the effect on the transmitted constellations of all the components that have been expounded in this Chapter, apart from the interference. Thus the scatter plot is performed taking into account the transponder, the amplitude distortion and the phase noise. Additive white gaussian noise (AWGN), uplink and downlink interferences are

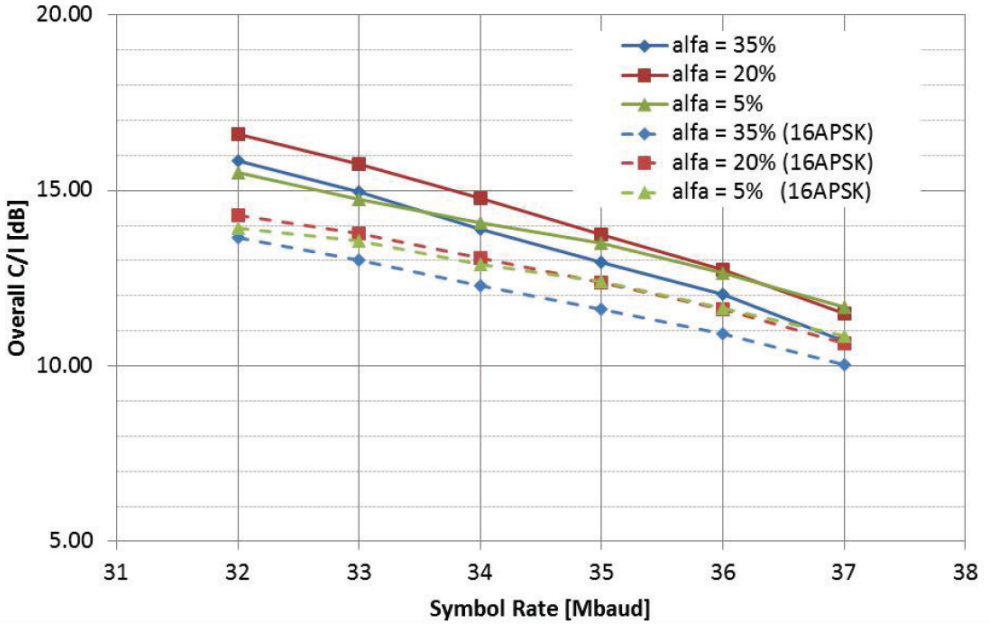

Figure 3.14: $\frac{C}{I}$ due to the transponder and uplink and downlink interferences

neglected in the pictures.

The modulations under test are 8APSK and 32APSK, like in the previous sections of this Chapter. The IBO values applied is quite high, like in Figure 3.9, $IBO = 10\,\text{dB}$, hence the HPA is working strongly in back-off, in the linear region.

For these kinds of constellations the working point is usually much closer to saturation, but we chose this parameter in order to have a clearer vision of the impairments. During the simulations these huge IBO values will be used only for very high order modulation like 64APSK, 128ASPK and 256APSK.

In Chapter 4 for every case we will examine which is the best IBO/OBO value in terms of PER. Then the transmitter can choose two paths: setting a certain IBO value finding a trade off between power loss and signal distortion, like we did for these scatter plot; or by mean of pre-distortion techniques choosing directly an OBO value and shaping the constellation trying to reduce the impact of the non-linear channel.

In the performance evaluation accomplished both these approaches will be used.

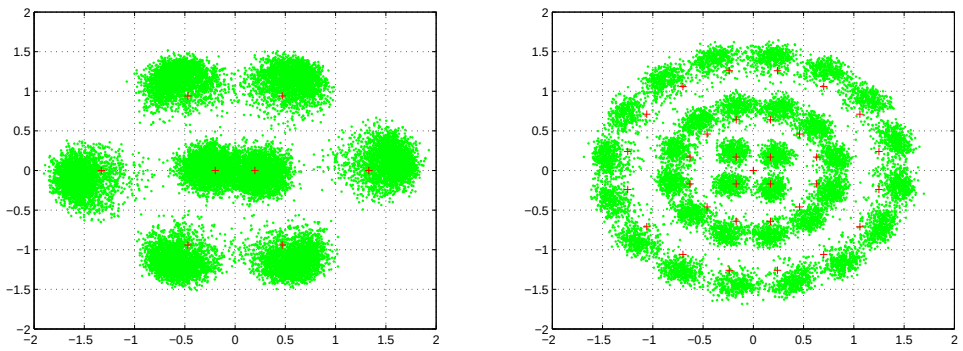

(a) (b)

Figure 3.15: (a) Scatter plot of 8APSK filtered by all the satellite channel, (b) Scatter plot of 32APSK filtered by all the satellite channel

Chapter 4

Performance over Satellite Channels

The following chapter presents a performance evaluation of the DVB-S2X standard over three models of satellite channel, that can be applied in different scenarios, and are presented in [15]. These performance give just an idea on how the standard operates, but fluctuations on the efficiency can be present, due to differences in the design.

The three scenarios taken into consideration are: Direct to Home (DTH), Very Small Aperture Terminal (VSAT) and Digital Satellite News Gathering (DSNG) scenario. These schemes correspond to different kinds of applications:

- **DTH**: it is a broadcast scenario, that accomplishes the distribution of digital multi-programme Television, and HDTV.
- **VSAT**: it is a multi-carrier scenario where six signals per transponder are expected. This corresponds to a situation in which there are multiple users that can for instance establish an IP connection
- **DSNG**: this is a multi-carrier scenario as well, but with only two carriers per transponder. This setting is often used in news gathering that consists in point-to-point, or point-to-multipoint transmission with stable or moving Earth stations.

In Section 4.1 will be examined the DTH scenario, in Section 4.2 the VSAT one, and finally in 4.3 the DSNG setting.

4.1 DTH channel

4.1.1 Channel scheme

DTH scenario, shown in Figure 4.1, is basically composed of three different Earth stations that generate different uplink signals. In the simulation it is sufficient to generate only a PN sequence, and delay it in order to diminish the correlation between the three inputs. In the Earth segment an HPA is present, but it will be neglected in the simulations, since we will assume a huge value of available power, therefore the amplifier is going to have a working point in the linear region, thus does not introduce high degradation. The other carriers are then shifted by a frequency f_T, since they occupy other bandwidths, and follow the same procedure of the carrier under test, therefore the ground amplifier will be neglected for them as well. In the scheme is also provided an uplink attenuation, in order to test the worst case situation in which the carrier under test has a power impairment due to atmosphere and rain attenuation, and other interfering users have clear sky condition.

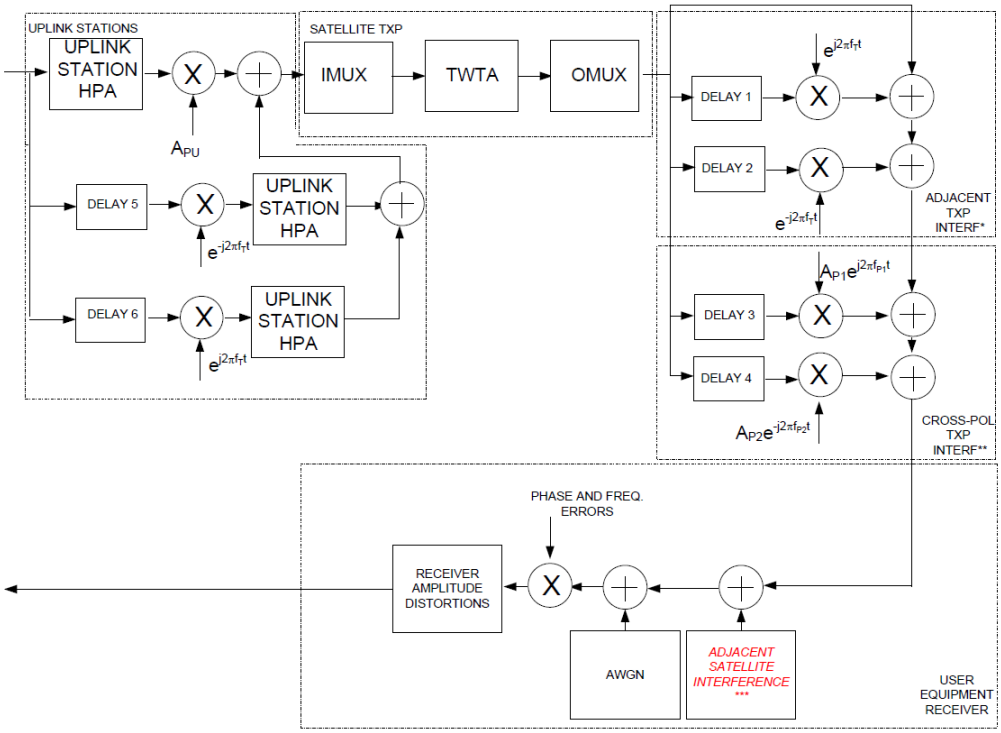

Figure 4.1: Block diagram of DTH channel

In the satellite segment we make use of a single transponder, where the carrier under test and the interference components are amplified together. The TWTA, IMUX and OMUX models used are the one presented in Chapter 3, specifically the ones in Figures 3.3, 3.4, and 3.5, they have bandwidth of 36 MHz. The useful carrier is a 34 MHz signal with roll-off $\alpha = 0.2$ or $\alpha = 0.05$, and it is the transponder input along with the side components of the carriers belonging to other channels.

In downlink the scheme presents mainly two contributions, which are from the adjacent carriers, and the cross-polar interference. The two adjacent carriers are the downlink replica of the aforementioned signals in uplink, thus in the simulation environment they are frequency shifted by the spacing frequency f_T, and they are delayed for correlation reasons, like in the uplink segment. The Cross-Polar interference is due to the satellite antenna polarization discrimination, the depolarization due to the atmospheric channel and the terminal antenna polarization discrimination. As far as the interference scenario is concerned, in Figure 4.2 is shown the pattern of the carrier under test and the interfering signals.

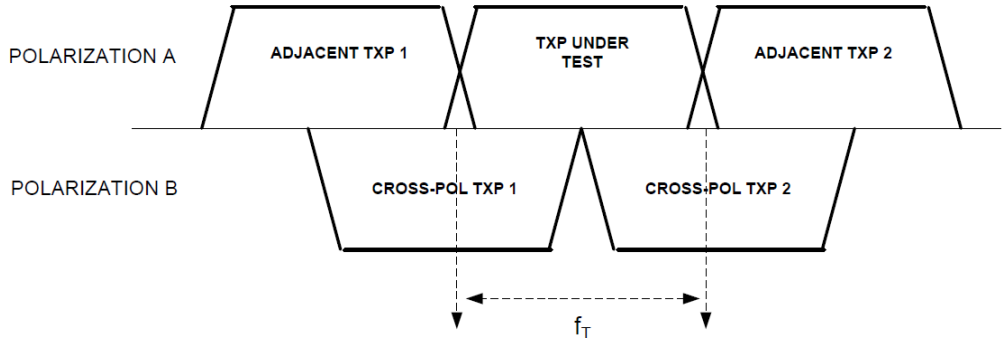

Figure 4.2: DTH interference pattern

Finally the last components of the scenario are adjacent satellite interference, which is optional and has been neglected in the simulations, AWGN block, and the impairments due to the LNB and the cable which are phase noise and amplitude distortion.

The phase noise mask used in DTH scenario, have been taken by state of the art and older equipment. And the uplink, downlink, and satellite payload contributions have been taken into account. The slope of different phase noise masks is shown in 4.3, but we are reducing to only two masks which are pointed out in 4.4.

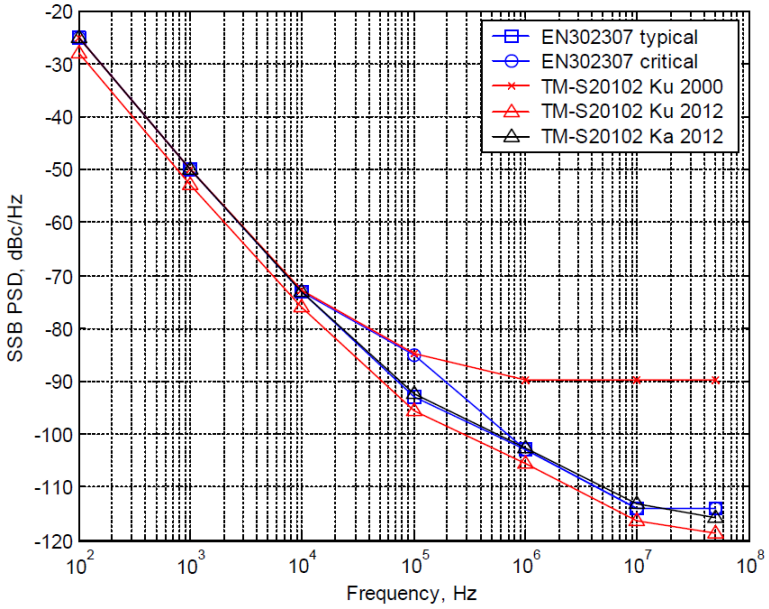

Figure 4.3: Phase noise masks for DTH scenario

Masks	100 Hz	1 kHz	10 kHz	100kHz	1MHz	10 MHz	≥50 MHz
P1 mask SSB dBc/Hz	-25	-50	-73	-92.25	-102.49	-113.23	-115.89
P2 symbol rates less than 36 Mbaud SSB dBc/Hz	-25	-50	-72.90	-84.76	-89.68	-89.68	-89.68

Figure 4.4: Phase noise mask values for DTH scenario

4.1.2 Simulation setting

DTH scenario simulation will be accomplished making use of many different MODCODs. Twenty-six different transmission settings will be tested, which correspond to 13 MODCODs and 2 different roll-off values:

- QPSK modulation with code rate 13/45, 1/2 and 3/4;
- 8PSK modulation with code rate 3/5, 25/36, 3/4 and 5/6;
- 16APSK modulation with code rate 26/45, 2/3, 3/4 and 77/90;
- 32APSK modulation with 32/45 and 4/5;

Higher order modulations will not be tested in this scenario, because they are not widely used in broadcast systems.

The considered frame length will be the long one $\eta = 64800$ bit, however the performance for the short one should have similar shape, but shifted by nearly $0.2 - 0.3$ dB.

As said before the baud rate will be $B = 34$ MHz, with roll-off $\alpha = 0.2$ and $\alpha = 0.05$, and the transponder bandwidth $B_w = 36$ MHz. The phase noise mask used will be P1 from Figure 4.4, and a power unbalance of $A = -8$ dB in uplink can be applied to the carrier under test in some cases.

In this scenario IBO/OBO optimum values were already available by previous simulations, instead in the following channel schemes some tests will be performed in order to find the best parameters. In table 4.1 the simulation settings are listed.

Modulation	Code rate	Baud Rate and Roll off	OBO
QPSK	13/45, 1/2, 3/4	34 Mbaud, $\alpha = 0.2$	1 dB
QPSK	13/45, 1/2, 3/4	34 Mbaud, $\alpha = 0.05$	1 dB
8PSK	3/5, 25/36, 3/4, 5/6	34 Mbaud, $\alpha = 0.2$	1 dB
8PSK	3/5, 25/36, 3/4, 5/6	34 Mbaud, $\alpha = 0.05$	1 dB
16APSK	26/45, 2/3, 3/4, 77/90	34 Mbaud, $\alpha = 0.2$	1.5 dB
16APSK	26/45, 2/3, 3/4, 77/90	34 Mbaud, $\alpha = 0.05$	1.75 dB
32APSK	32/45, 4/5	34 Mbaud, $\alpha = 0.2$	2.5 dB
32APSK	32/45, 4/5	34 Mbaud, $\alpha = 0.05$	2.5 dB

Table 4.1: Simulation parameters for DTH scenario

After parameters setting a pre-distortion technique will be applied in this scenario . Like is explained in [14] the idea is setting the decoding procedure on the distorted constellation points detected as output of the satellite channel. There are two types of the pre-distortion, which are static and dynamic. The static one proceeds iteratively generating S blocks of W symbols, computing the error at the end of each block and updating the points. This procedure is a loop that allows to find the pre-distorted values. This can be achieved by mean of a least mean square (LMS) algorithm as following:

$$\rho_c^{(n)}(s)\, e^{j\theta_c^n(s)} = \frac{1}{W} \sum_{k \in l^{(n)}, sW+1 \leq k \leq (s+1)W} z(k) \qquad n = 1, .., M, s = 1, ...S \tag{4.1}$$

equation 4.1 shows the calculation of the constellation point. $\rho_c^{(n)}(s)$ is the modulus of the point, $\theta_c^n(s)$ the phase, s is the current step of the algorithm, $z(k)$ is the complex output that we examine after the satellite channel, and $l^{(n)}$ is the reference constellation point. Afterward the error function will be evaluated, which is given by

$$e^{(n)}(s) = \rho_c^{(n)}(s)\, e^{j\theta_c^n(s)} - c_{TX}^{(n)} \tag{4.2}$$

where $c_{TX}^{(n)}$ is the reference constellation point, and $e^{(n)}(s)$ is the error at step s on the point n. The following step is updating the modulus and the argument with a rate respectively γ_ρ and γ_θ. The improvement of the parameters is the following:

$$\rho_{c_{TX}}^{(n)}(s+1) = \rho_{c_{TX}}^{(n)}(s) - \gamma_\rho \left| e^{(n)}(s) \right| \tag{4.3}$$

$$\theta_{c_{TX}}^{(n)}(s+1) = \theta_{c_{TX}}^{(n)}(s) - \gamma_\theta \psi(s) \tag{4.4}$$

given that $\psi(s)$ is defined in this manner

$$\psi(s) = \begin{cases} arg\left(e^{(n)}(s)\right) - 2\pi, & for \quad arg\left(e^{(n)}(s)\right) > \pi \\ arg\left(e^{(n)}(s)\right) + 2\pi, & for \quad arg\left(e^{(n)}(s)\right) < -\pi \\ arg\left(e^{(n)}(s)\right), & otherwise \end{cases} \tag{4.5}$$

The dynamic pre-distortion instead considers the channel memory, thus it constructs a table with all the possible L symbols (counting precursors and post-cursors) and applies a pre-distortion by mean of offline simulations, with the optimum OBO value.

4.1.3 Performance evaluation

The performance evaluation will be accomplished focusing on two different outcomes, which are the PER and the spectral efficiency of the MODCODs versus the P_{SAT}/N_0 that allows the desired error thresold, which in our case is $PER = 10^{-5}$. P_{SAT}/N_0 term is related to SNR, but it takes also into account the power lost working in back-off, and it is given by

$$P_{SAT}/N_0 = \frac{(E_s R_s)\, OBO}{N_0 B_w} \tag{4.6}$$

where E_s is the symbol energy, R_s the baud rate, OBO is the OBO value in linear, N_0 is the power spectral density of the noise and B_w the reference bandwidth.

As far as spectral efficiency is concerned, it will be calculated using

$$\eta = \eta_M \frac{R_s}{B_w} \tag{4.7}$$

where η_M is the efficiency of the MODCOD in bits/symbol and, as before, R_s is the Baud Rate and B_w the reference bandwidth.

Defined the mathematical terms it is possible to examine the outcomes of the computer simulations. The PER trend versus P_{SAT}/N_0 is shown in Figures 4.5 and 4.6 for roll-off $\alpha = 0.2$, 4.7 and 4.8 for $\alpha = 0.05$.

In this scenario, as the diagrams show, the attenuation in uplink does not seem to be a huge problem. As a matter of fact the MODCODs performance with power unbalance are almost the same of the ones without, actually with roll-off $\alpha = 0.05$ the two curves are almost exactly overlapped. This is true because the transponder is used in single carrier mode, thus the lost power in uplink is recovered by the HPA without any drawbacks. But, as we will examine in Section 4.3, if the transponder operates in a multi-carrier mode this issue is more problematic, and brings to a performance degradation proportional to the MODCOD used.

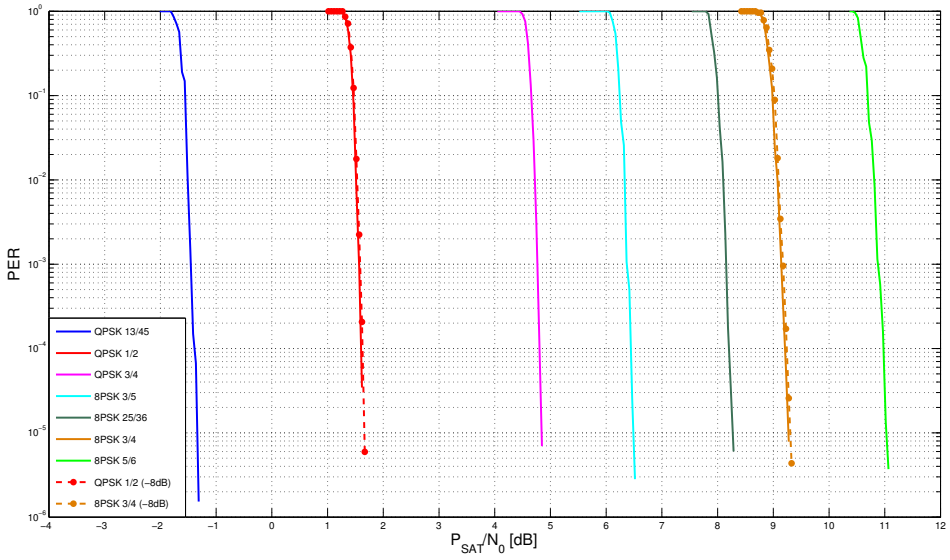

Figure 4.5: Packet error rate of the lowest order MODCODs in DTH scenario with $\alpha = 0.2$

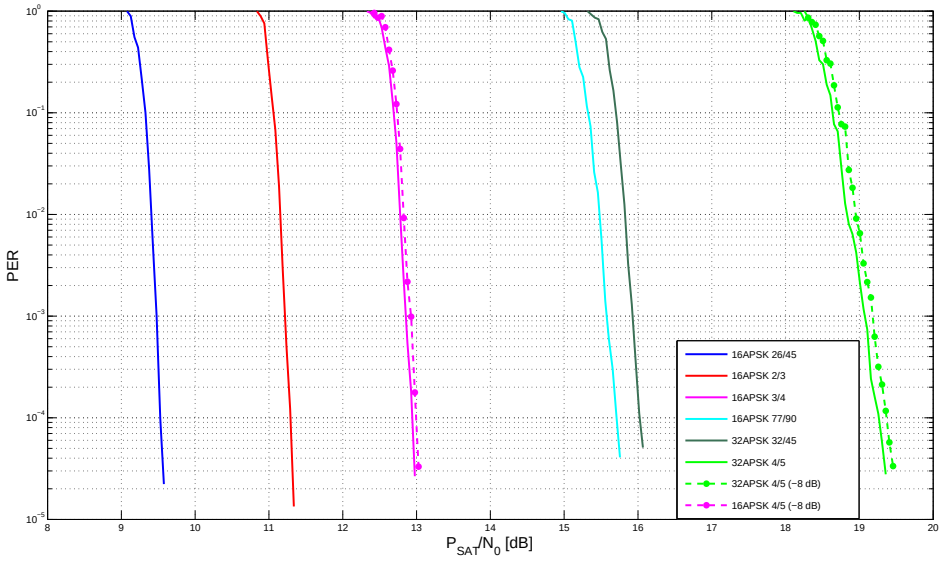

Figure 4.6: Packet error rate of the highest order MODCODs in DTH scenario with $\alpha = 0.2$

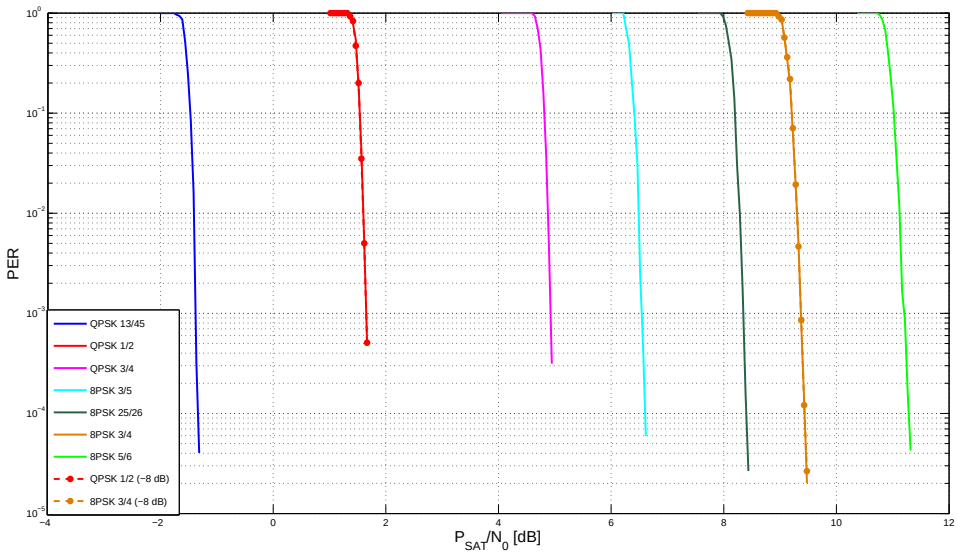

Figure 4.7: Packet error rate of the lowest order MODCODs in DTH scenario with $\alpha = 0.05$

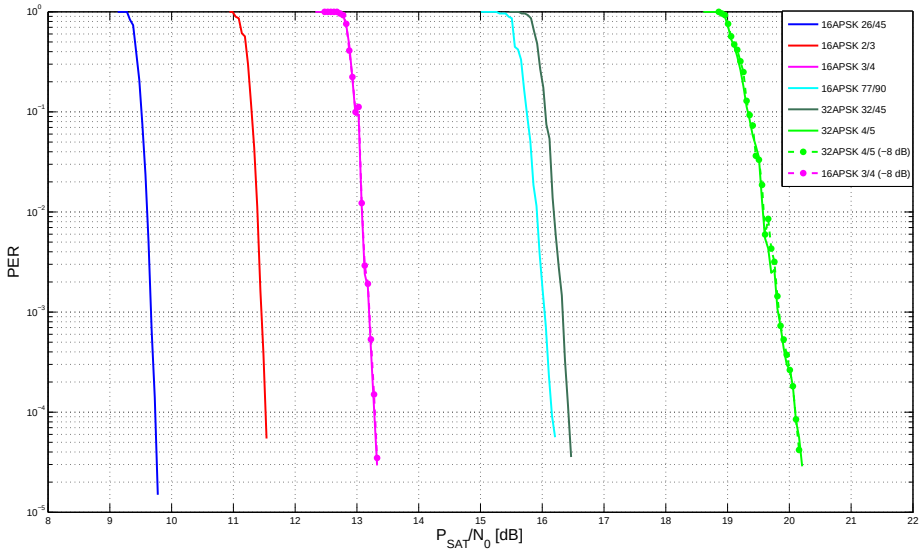

Figure 4.8: Packet error rate of the highest order MODCODs in DTH scenario with $\alpha = 0.05$

Diagrams 4.5, 4.6, 4.7 and 4.8 display that in terms of PER, comparing the two roll-off modes, the roll-off 20% one performs slightly better, because its waterfall region is nearly 0.5 dB before the one with roll-off 5%. This difference changes lightly depending on the MODCOD.

After these considerations we expect that in terms of spectral efficiency the roll-off $\alpha = 0.2$ transmission setting performs better, because both transmission modes use the same Baud Rate, thus the only variable is the value of P_{SAT}/N_0 needed for the error threshold. Figure 4.9 shows that what we stated is true.

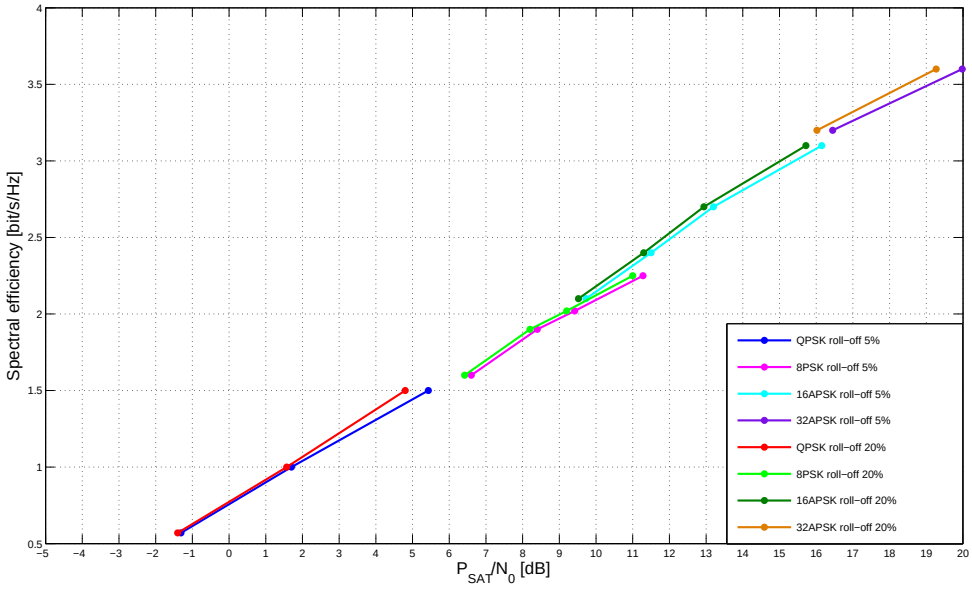

Figure 4.9: Spectral efficiency on DTH scenario

4.2 VSAT channel

4.2.1 Channel scheme

VSAT channel is a multi-beam scenario designed to feed multiple users. The satellite transponder is working in a multi-carrier mode. In this case is taken into account a two beams transmission, with three carriers per beam, therefore we have six different carriers as transponder input.

In the uplink scheme there are six users which transmit a signal to the satellite payload. Like in the DTH case it is possible to generate a single PN sequence, and perform a delay on it, in order to eliminate correlation. The frequency space f_C between the carriers is set to 75 Mhz, and the one between the beams f_B is 225 MHz. Hence after the uplink signals generation every sequence is frequency shifted by a value which leads to a representation accordant to Figure 4.11. All these signals are summed up and will generate the satellite transponder input.

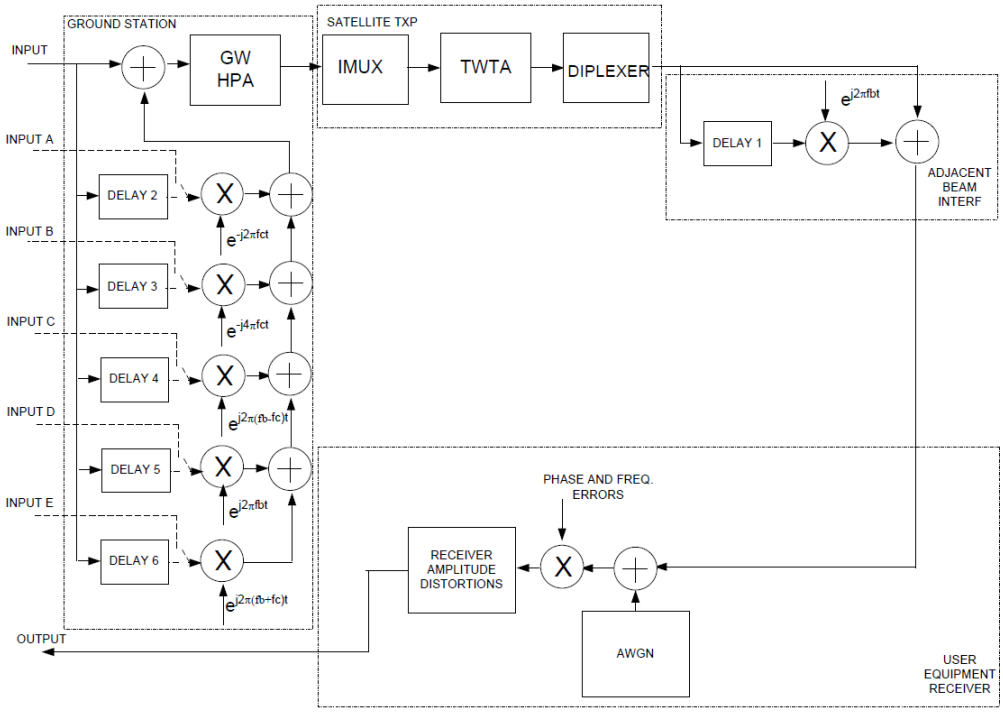

Figure 4.10: Block diagram of VSAT channel

In the satellite payload a 500 MHz transponder is simulated. Six different carriers enter the IMUX and are then amplified by TWTA. After the HPA

the two beams are divided by a 250 MHz diplexer, which acts like a double OMUX that applies "channelization" [19].

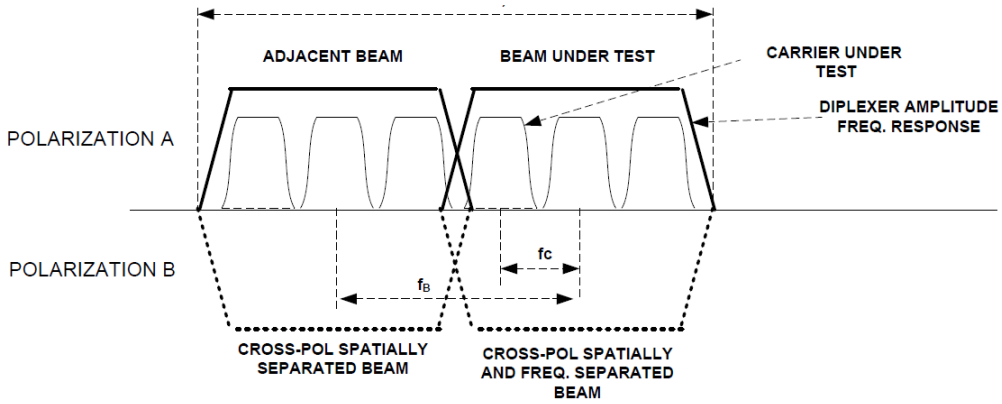

Figure 4.11: VSAT frequency scheme

In the downlink section is performed only the inter-beam interference, so a non-correlated sequence is summed to the beam under test, with frequency spacing f_B.

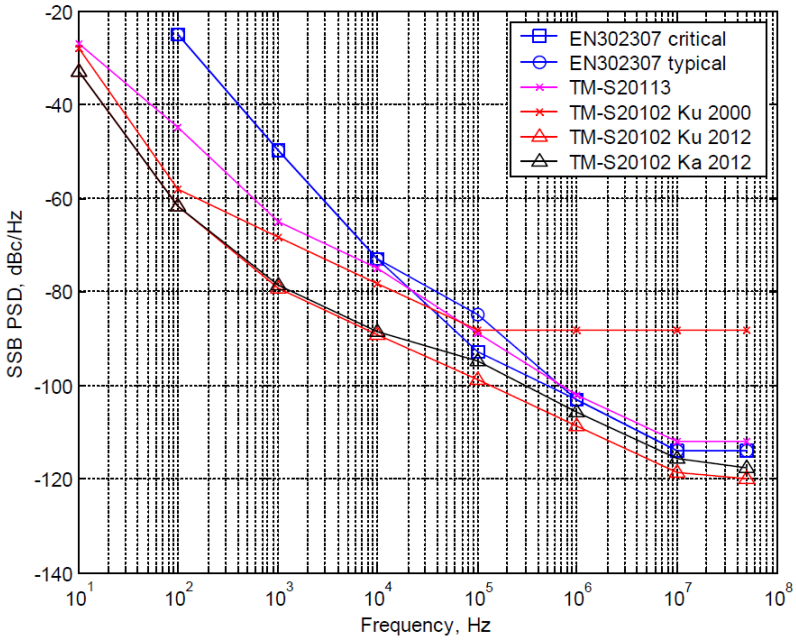

Figure 4.12: Phase noise masks for non DTH scenario

AWGN is then introduced in the system along with the cable distortion, and the phase noise. For the latter different phase noise masks are used, due

to the different kinds of services. Like in the previous case in Figure 4.12 is shown a trend of the different phase noise masks taken from state of the art and old equipment, and in Figure 4.13 are expounded the values used in the simulations.

Masks	10 Hz	100 Hz	1 kHz	10 kHz	100kHz	1MHz	10 MHz	≥50 MHz
P1 mask SSB dBc/Hz	-27	-45	-65	-75	-89	-102	-112	-112
P2 mask SSB dBc/Hz	-32.93	-61.96	-78.73	-88.73	-94.83	-105.74	-115.74	-117.74

Figure 4.13: Phase noise mask values for non DTH scenario

4.2.2 Simulation setting

In Very Small Aperture Terminal scenario several MODCODs are going to be tested. In this scheme the transmission settings achieve higher spectral efficiency, and the user has higher bandwidth available, therefore the data rate is going to be much higher. The spectral efficiency is due to the use of higher order modulations, until 128APSK. The bandwidth values that are going to be applied are 60 MHz with roll-off $\alpha = 0.2$, and 70 MHz using roll-off $\alpha = 0.05$.

The satellite transponder is, as said in the previous section, a 500 MHz with a 250 MHz diplexer on the output section, in order to split the two beams that are going to be transmitted. The TWTA model is the linearized one, shown in Figures 3.6 and 3.7, and the phase noise mask set is the one presented in last section, Figures 4.12 and 4.13.

Two different packet lengths will be taken in account: the long one, with length $\eta = 64800$ bit, for every "L" MODCOD, and for the highest order modulation (128APSK). And the short one, $\eta = 16200$, for all the other MODCODs that are going to be tested.

Therefore the constellations analyzed in the computer simulations are the following, with the related code rate:

- QPSK modulation with code rate 1/4, 1/2 and 3/4;
- 8PSK modulation with code rate 3/5 and 3/4;
- 8PSK-L modulation with code rate 5/9 and 26/45;
- 16APSK modulation with code rate 2/3;
- 16APSK-L modulation with code rate 2/3 and 5/9;

- 32APSK and 32APSK-L modulations with code rate 2/3;
- 64APSK-L modulation with code rate 32/45;
- 128APSK modulation with code rate 3/4.

Now that all the simulation parameters are set, the first step is setting the optimum IBO/OBO value on the signal amplified by the transponder, in order to minimize the distortion and the inter-modulation products, and hence have the best performance possible in this kind of scenario. For finding out the optimum values for every modulation, a quite empirical method has been used: a SNR value at the beginning of the waterfall region has been chosen, than the PER has been evaluated for several values of IBO/OBO, and finally the HPA working point that gave best results in term of errors has been set for the MODCODs which use the modulation under test.

In Figures 4.14 and 4.15 the slope of PER in function of the OBO values is shown for both roll-offs, thus now we can set the optimum TWTA working point for every MODCOD.

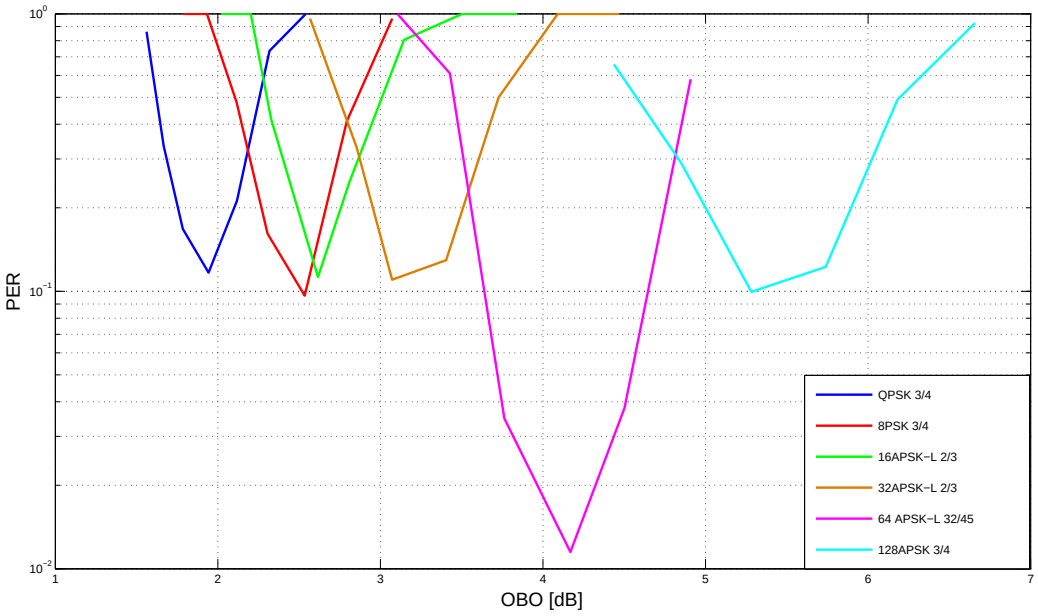

Figure 4.14: PER in function of OBO value in the waterfall region for roll-off $\alpha = 0.2$

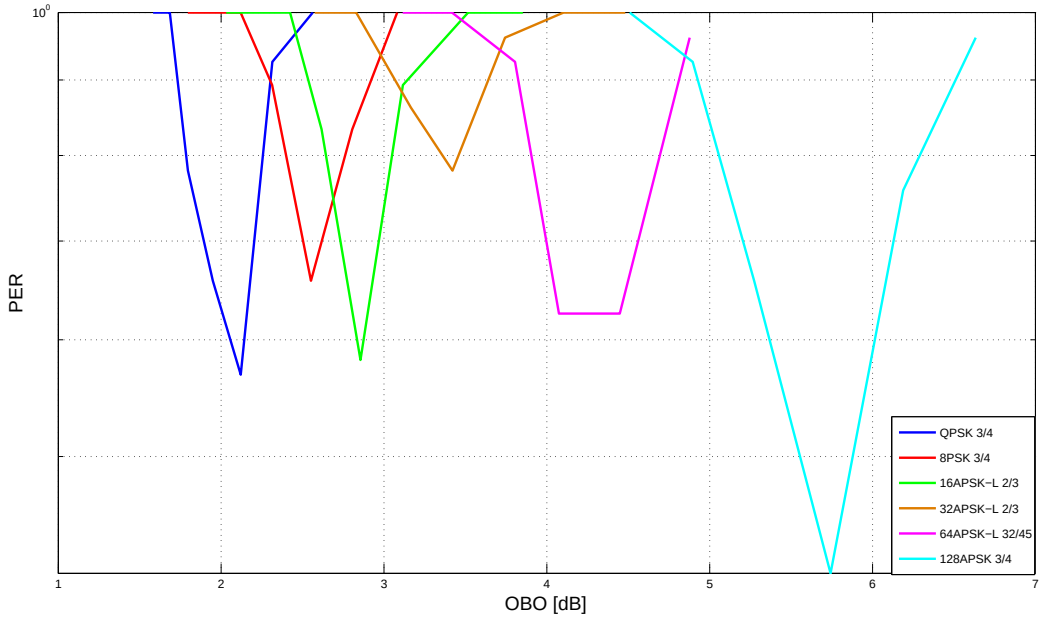

Figure 4.15: PER in function of OBO value in the waterfall region for roll-off $\alpha = 0.05$

In Table 4.2 it is possible to examine the SNR gaps from the Quasi-Error-Free status in AWGN in which these simulations are performed.

Modulation	SNR Gap from AWGN
QPSK 3/4	2.9 dB
8PSK 3/4	3.5 dB
16APSK-L 2/3	3.8 dB
32APSK-L 2/3	4.65 dB
64APSK-L 32/45	5.75 dB
128APSK 3/4	8.05 dB

Table 4.2: SNR gap from AWGN QEF used in the OBO optimum simulations in VSAT scenario

Finally, from the diagrams in Figures 4.14 and 4.15, we can set the simulation parameters choosing the optimum values of IBO/OBO for every modulation. Thus to every MODCOD which employs a certain constellation will

be applied the IBO/OBO found from the aforementioned simulations, taking into account the roll-off value used as well.

In table 4.3 are summarized the simulation parameters applied in the VSAT scenario.

Modulation	Code rate	Baud Rate and Roll off	IBO	OBO
QPSK	1/4, 1/2, 3/4	60 Mbaud, $\alpha = 0.2$	1.5 dB	1.94 dB
QPSK	1/4, 1/2, 3/4	70 Mbaud, $\alpha = 0.05$	2 dB	2.12 dB
8PSK	3/5, 3/4	60 Mbaud, $\alpha = 0.2$	3 dB	2.53 dB
8PSK	3/5, 3/4	70 Mbaud, $\alpha = 0.05$	3 dB	2.53 dB
8PSK-L	5/9, 26/45	60 Mbaud, $\alpha = 0.2$	3 dB	2.53 dB
8PSK-L	5/9, 26/45	70 Mbaud, $\alpha = 0.05$	3 dB	2.53 dB
16APSK-L	5/9, 2/3	60 Mbaud, $\alpha = 0.2$	3 dB	2.61 dB
16APSK-L	5/9, 2/3	70 Mbaud, $\alpha = 0.05$	3.5 dB	2.86 dB
16APSK	2/3	60 Mbaud, $\alpha = 0.2$	3 dB	2.61 dB
16APSK	2/3	70 Mbaud, $\alpha = 0.05$	3.5 dB	2.86 dB
32APSK-L	2/3	60 Mbaud, $\alpha = 0.2$	4 dB	3.07 dB
32APSK-L	2/3	70 Mbaud, $\alpha = 0.05$	4.5 dB	3.42 dB
32APSK	2/3	60 Mbaud, $\alpha = 0.2$	4 dB	3.07 dB
32APSK	2/3	70 Mbaud, $\alpha = 0.05$	4.5 dB	3.42 dB
64APSK-L	32/45	60 Mbaud, $\alpha = 0.2$	5.5 dB	4.17 dB
64APSK-L	32/45	70 Mbaud, $\alpha = 0.05$	5.5 dB	4.07 dB
128APSK	3/4	60 Mbaud, $\alpha = 0.2$	7 dB	5.28 dB
128APSK	3/4	70 Mbaud, $\alpha = 0.05$	7.5 dB	5.74 dB

Table 4.3: Simulation parameters for VSAT scenario

From these results it can be noticed that, as explained in Chapter 3, more the modulation order is high, more we need to work in back-off.

4.2.3 Performance evaluation

The performance evaluation consists on the PER calculation over P_{SAT}/N_0, defined like in 4.6.

Afterward, found the PER values and QEF threshold for every MODCOD, it is possible to plot the trend of the spectral efficiency in function of P_{SAT}/N_0.

The simulation loop generates different sequences and encode them using the designed MODCOD, subsequently applies the scheme described in Section 4.2.1, and generates the two beams spectrum plotted in Figure 4.16.

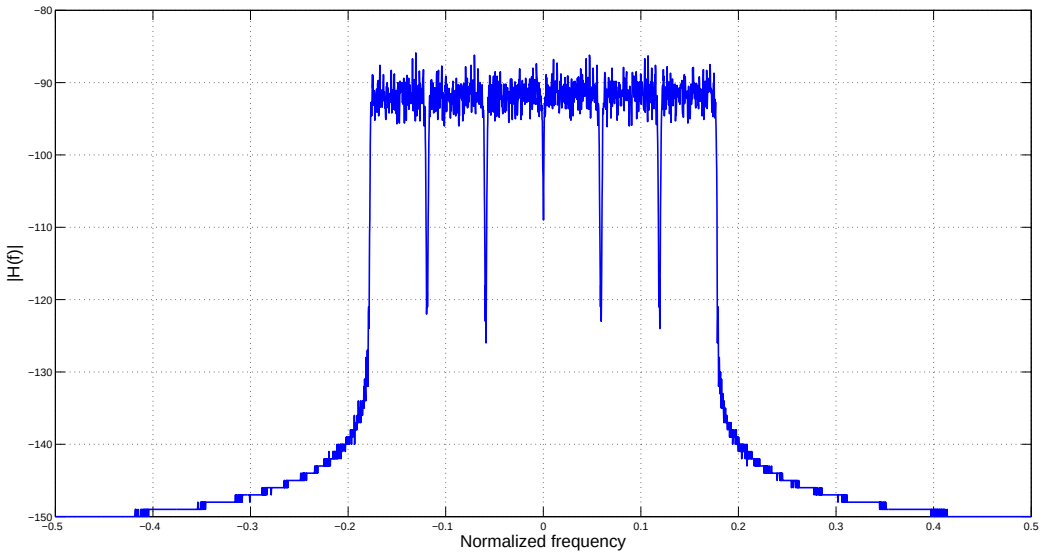

Figure 4.16: Normalized spectrum of the two beams in VSAT scenario

The power in Figure 4.16 is normalized to one, like in the DTH simulation environment. We must remind that the maximum power of the signal in after the satellite transponder is equal to one (0 dB), and if the system is in back-off the transmitted power will be negative in dB. In fact AWGN is generated with respect to normalized power.

Given these assumptions, PER can be evaluated over P_{SAT}/N_0. In Figures 4.17 and 4.18 it is plotted for roll-off $\alpha = 0.2$, and in 4.19 and 4.20 for $\alpha = 0.05$.

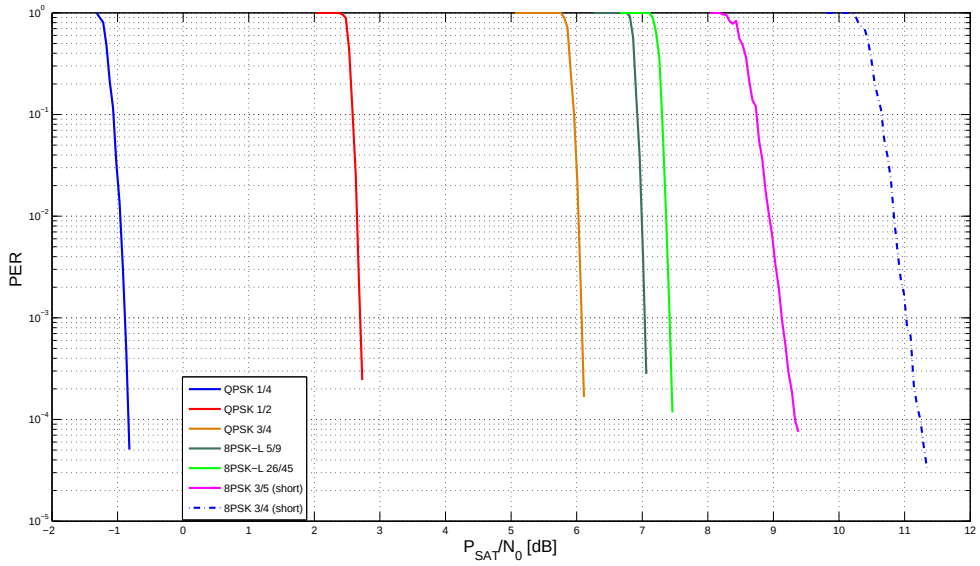

Figure 4.17: Packet Error Rate of the lowest order MODCODs in VSAT scenario with $\alpha = 0.2$

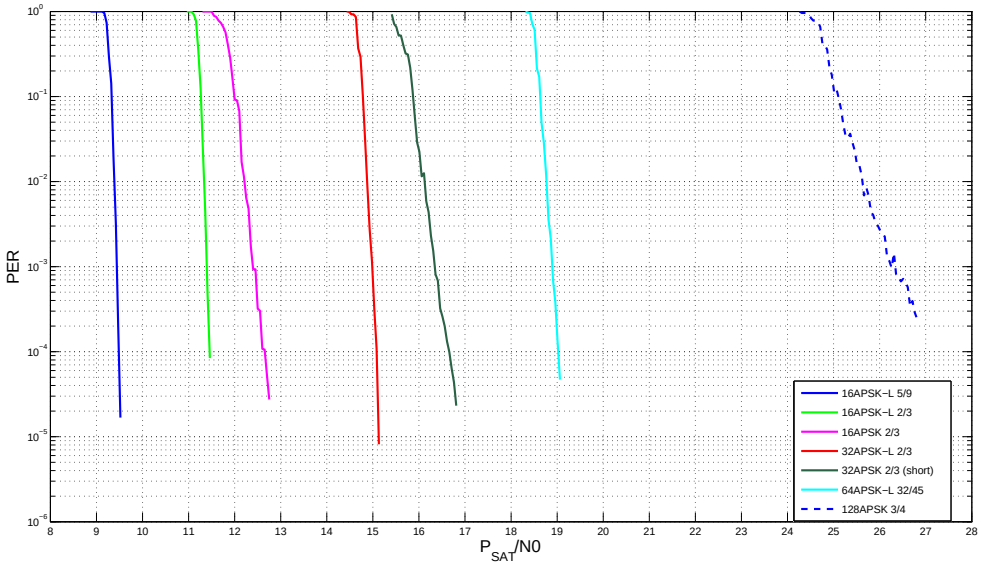

Figure 4.18: Packet Error Rate of the highest order MODCODs in VSAT scenario with $\alpha = 0.2$

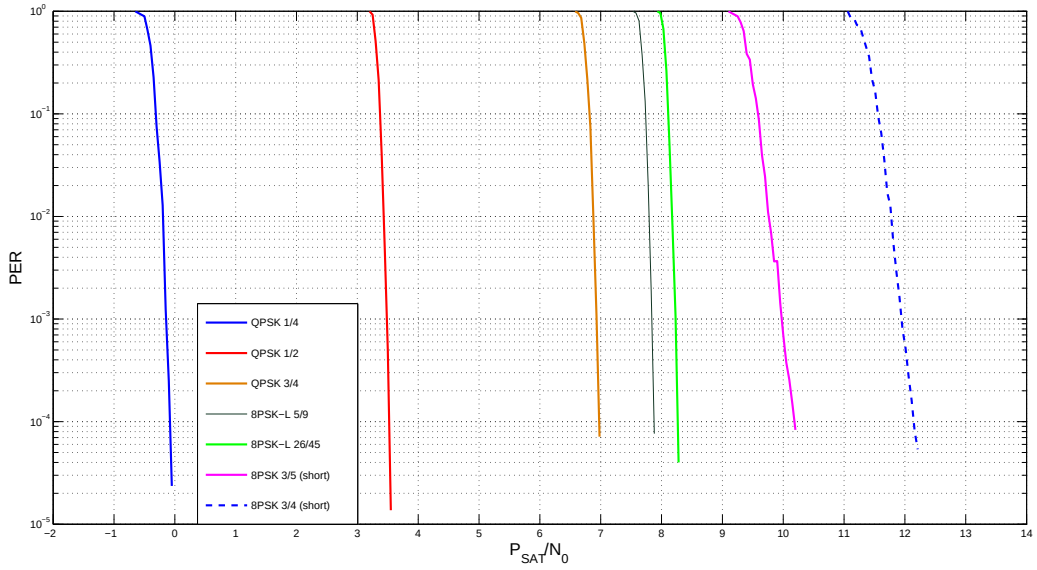

Figure 4.19: Packet Error Rate of the lowest order MODCODs in VSAT scenario with $\alpha = 0.05$

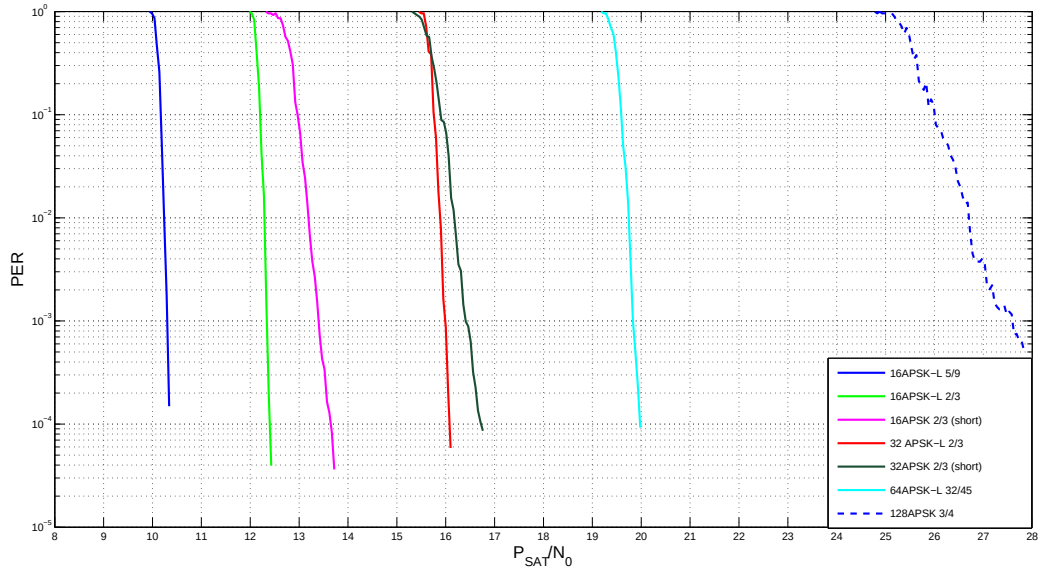

Figure 4.20: Packet Error Rate of the highest order MODCODs in VSAT scenario with $\alpha = 0.05$

In VSAT scenario, from the outcomes, it can noticed that first the highest order modulation that has been run is really bad performing, because its PER decreases for really high SNR levels, and with very low slope, unlike the other MODCODs which reduce their PER in the waterfall region in an interval usually around 0.5 dB.

Afterward performance degradation is present when the short packet length MODCODs are used. Focusing on 8PSK, 16APSK and 32APSK, the long packet version performs much better than the short one. For 8PSK this is due to the use of an higher code rate, but generally, thanks to the "L" version modulation and to long frame, we can achieve higher performance, as stated in Chapter 2.

Finally in terms of PER from the diagrams we note that roll-off $\alpha = 20\%$ performs better, because the waterfall region of every MODCOD is slightly translated to lower P_{SAT}/N_0 values. However, for the overall system performance, taking into account the spectral efficiency given by 4.7, we must remind that the $\alpha = 5\%$ version has an higher Baud Rate available, which is 70 MHz instead of 60 MHz. The diagram with the spectral efficiency trend for this scenario is shown in figure 4.21.

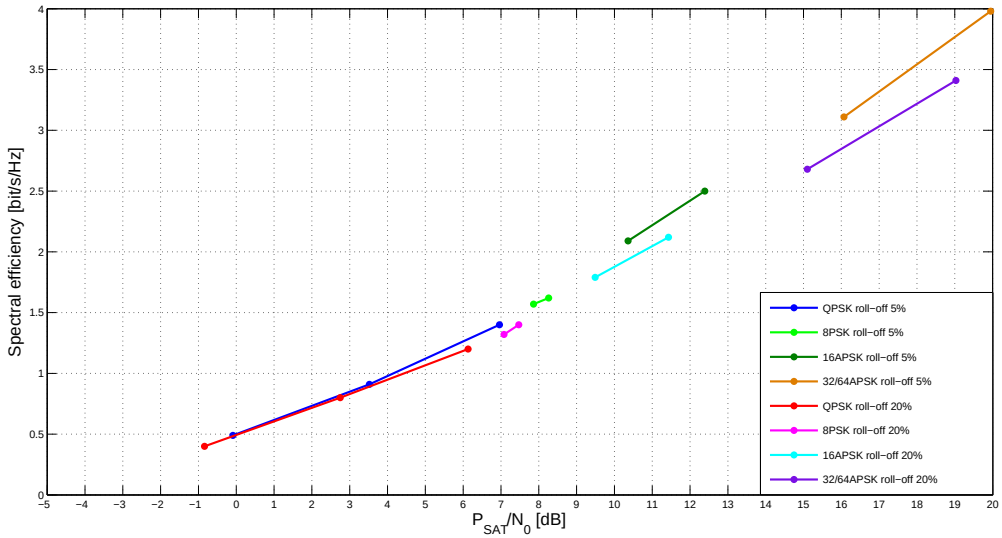

Figure 4.21: Spectral efficiency for VSAT scenario

Therefore $\alpha = 0.05$ setting performs better thanks to the higher symbol rate, even though the PER value with the same P_{SAT}/N_0 condition is higher

with respect $\alpha = 0.2$. Unfortunately in this kind of scenario we cannot make use of the same baud rate for both values of roll-off like in the DTH one. This is due to interference matters, since the first was a single carrier scheme, thus it was possible pushing more symbol rate without any degradation, but in this case we would cause huge interference between the carriers of the same beam.

4.3 DSNG channel

4.3.1 Channel scheme

The last channel model that we are going to simulate (Figure 4.22) is a typical DSNG scenario, in which two different signals are generated and both sent to the satellite transponder, with carrier spacing f_C. The interferent signal is a delayed copy of the one under test, like in the previous cases. The considered scenario is a worst case one, since an attenuation on the carrier under test of $A_{PU} = 4\,\text{dB}$ is applied, while the other carrier is in clear sky condition.

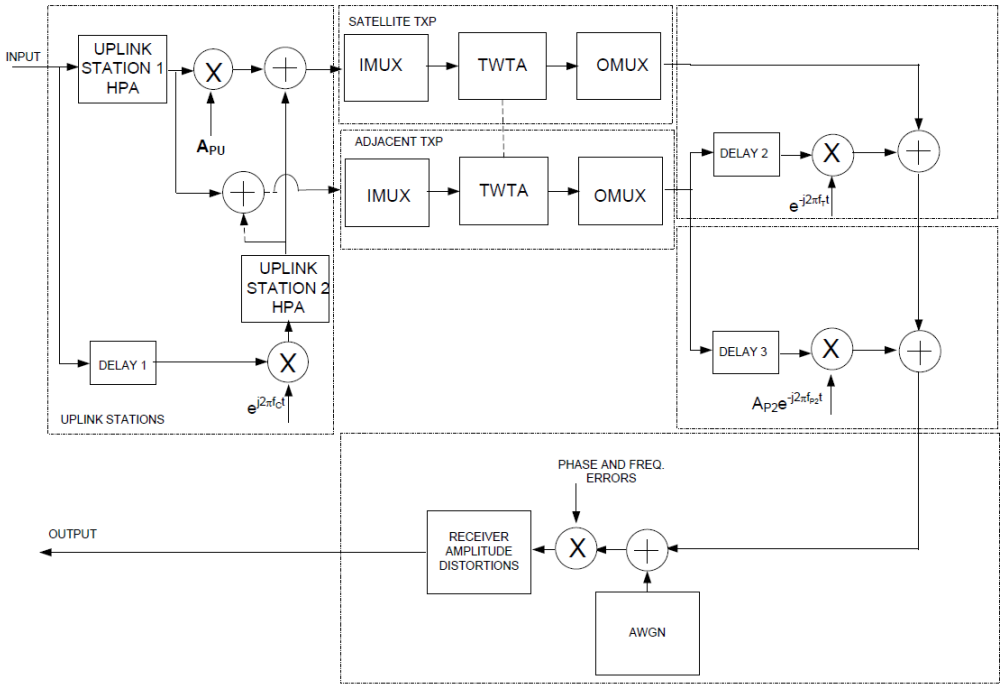

Figure 4.22: Block diagram of DSNG channel

The satellite payload will be characterized by two 36 MHz transponders. They will both be used in a two-carrier mode, since they will amplify both uplink signals.

In downlink there is an interference component given by the adjacent transponder, which has been delayed in order to introduce uncorrelation, and has been shifted by a value according to the transponder spacing frequency f_T. A cross-polar interference component is present as well. The resultant frequency scheme is shown in Figure 4.23.

Finally, at the end of the chain, there are AWGN, cable distortion, and

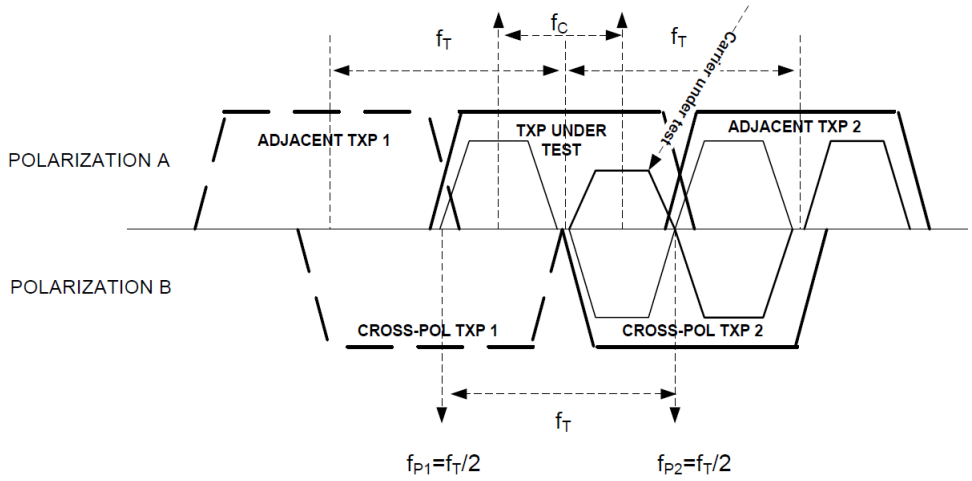

Figure 4.23: DSNG frequency scheme

phase noise. The phase noise mask used in this scenario is P2 mask of Figure 4.13.

4.3.2 Simulation setting

In this last scenario the simulations are focused on MODCODs up to 256APSK, therefore we are going to use all the modulation orders. The frame size will be set to long in every transmission setting. The constellations taken into account in DSNG channel model are:

- 8PSK-L modulation with code rate 5/9 and 26/45;
- 16APSK-L modulation with code rate 5/9 and 2/3;
- 32APSK-L modulation with code rate 2/3;
- 64APSK-L modulation with code rate 7/9;
- 128APSK modulation with code rate 3/4;
- 256APSK modulation with code rate 11/15.

The carriers Baud Rate is 15 MHz with roll-off $\alpha = 0.2$, and 17 MHz with $\alpha = 0.05$. The satellite transponder bandwidth is 36 MHz, and the model used is the same one applied in DTH scenario, hence the conventional one.

As far the IBO/OBO values are concerned a simulation similar to the one of Section 4.2 has been carried out.

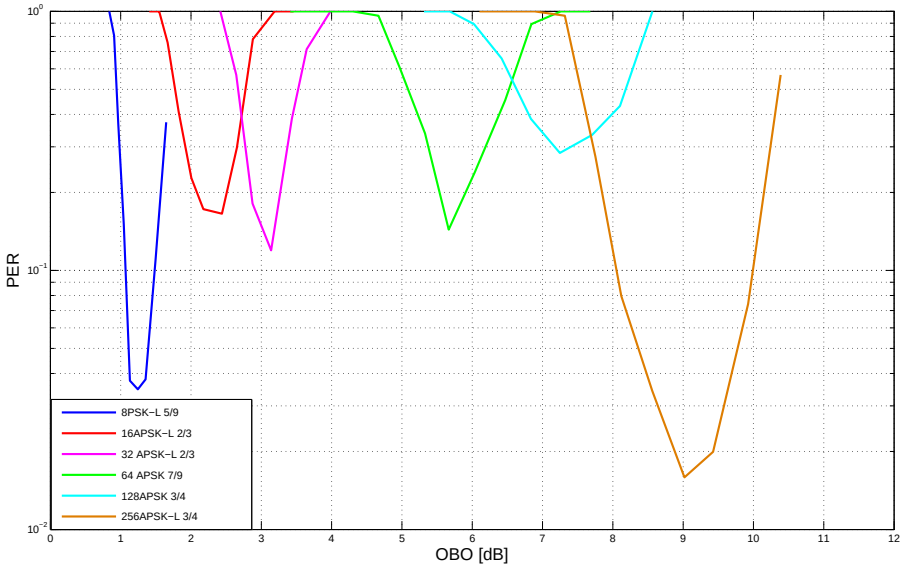

Figure 4.24: PER in function of OBO value in the waterfall region for roll-off $\alpha = 0.2$ in DSNG scenario

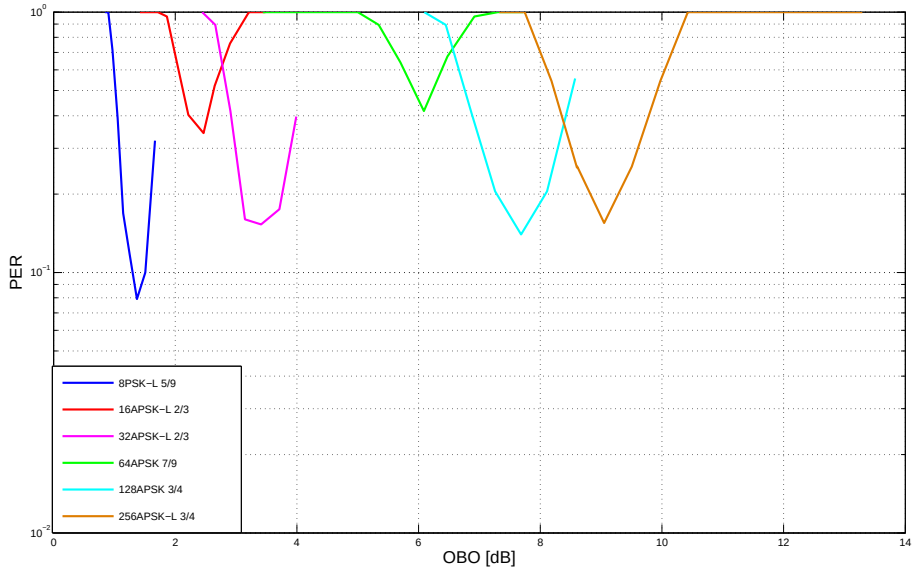

Figure 4.25: PER in function of OBO value in the waterfall region for roll-off $\alpha = 0.05$ in DSNG scenario

The diagrams have been traced with no power unbalance assumption, therefore no knowledge of the attenuation impairment in the system. In Figure 4.24 and Figure 4.25 are shown the trends of the PER in function of OBO respectively with roll-off 20% and 5%.

In order to examine the amount of the error estimating the IBO/OBO value in a scenario without power unbalance, a simulation with roll-off $\alpha = 0.05$ has been run with 4 dB power unbalance as well. Thus, in Figure 4.26, the PER trend is plotted taking into account the power unbalance on the carrier under test.

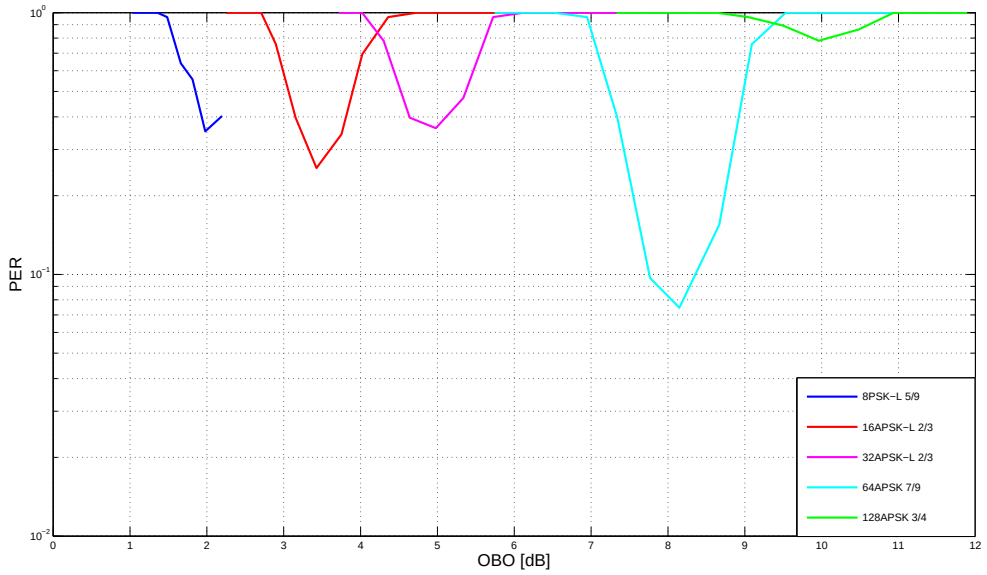

Figure 4.26: PER in function of OBO value in the waterfall region for roll-off $\alpha = 0.05$ in DSNG scenario with power unbalance

256APSK modulation has not been taken in consideration because, as we will find out in the outcomes exposition, it is not usable in a power unbalance scenario like the one that we are studying.

However comparing the diagrams in Figures 4.26 and 4.25, the shape of the curves are pretty similar, even though the optima OBO values are slightly different. Therefore, setting the IBO/OBO parameter assuming that the carrier under test is in clear sky condition when it is actually not, does not seem to bring a huge performance degradation. All these considerations are valid for roll-off $\alpha = 0.2$ as well.

In order to have a clue about the OBO error, in Figure 4.27, the OBO difference beetwen the power unbalance and clear sky scenario is plotted in

function of $log_2(M)$ where M is the modulation order.

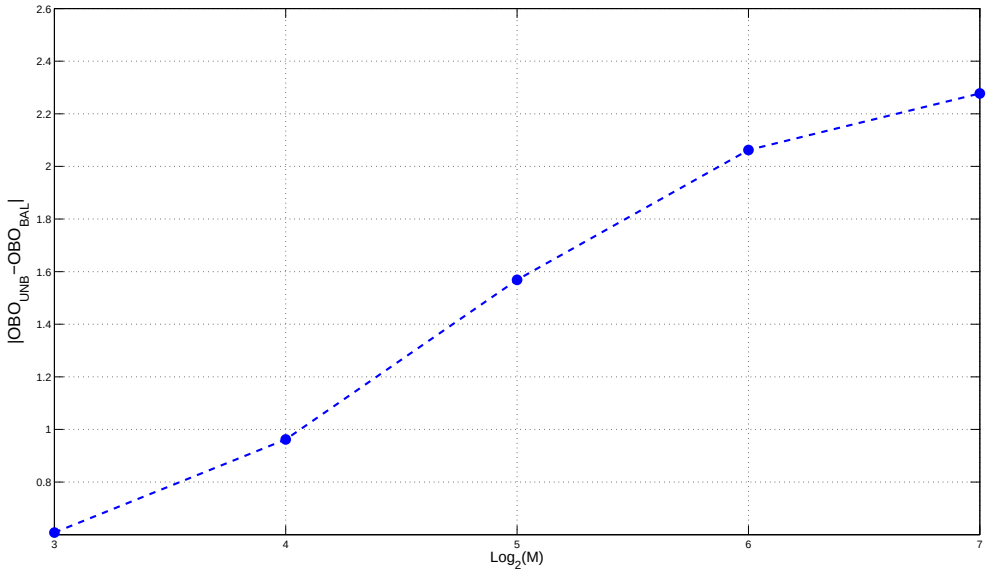

Figure 4.27: Absolute value of the OBO difference between power unbalance and clear sky scenario

As we expected the difference increases with the higher order modulations, so it reaches its maximum with 128APSK. In every case the IBO/OBO value is greater in the power unbalance case, this happens because the attenuation phenomenon introduces not only a reduction on the power under test, but leads to an higher degradation due to the inter-modulation products in the transponder. As a matter of fact the degradation caused by this impairment, as we will find out in the performance evaluation, can be more than just 4 dB.

Returning to the simulation parameters choice, as in Section 4.2, the SNR gap from the AWGN QEF threshold applied for the optimum OBO evaluation are reported in Table 4.4

Modulation	SNR Gap from AWGN
8PSK-L 5/9	2.7 dB
16APSK-L 2/3	4.1 dB
32APSK-L 2/3	5.35 dB
64APSK 7/9	8.5 dB
128APSK 3/4	10.5 dB
256APSK-L 3/4	12.8 dB

Table 4.4: SNR gap from AWGN QEF used in the OBO optimum simulations in DSNG scenario

Finally the parameter settings for the performance evaluation of DSNG channel model, given the previous considerations, are the ones expounded in Table 4.5.

Modulation	Code rate	Baud Rate and Roll off	IBO	OBO
8PSK-L	5/9, 26/45	15 Mbaud, $\alpha = 0.2$	2.5 dB	1.25 dB
8PSK-L	5/9, 26/45	17 Mbaud, $\alpha = 0.05$	3 dB	1.37 dB
16APSK-L	5/9, 2/3	15 Mbaud, $\alpha = 0.2$	6 dB	2.44 dB
16APSK-L	5/9, 2/3	17 Mbaud, $\alpha = 0.05$	6 dB	2.47 dB
32APSK-L	2/3	15 Mbaud, $\alpha = 0.2$	7.5 dB	3.14 dB
32APSK-L	2/3	17 Mbaud, $\alpha = 0.05$	8 dB	3.41 dB
64APSK	7/9	15 Mbaud, $\alpha = 0.2$	11.5 dB	5.67 dB
64APSK	7/9	17 Mbaud, $\alpha = 0.05$	12 dB	6.08 dB
128APSK	2/3	15 Mbaud, $\alpha = 0.2$	13.5 dB	7.25 dB
128APSK	2/3	17 Mbaud, $\alpha = 0.05$	14 dB	7.69 dB
256APSK-L	2/3	15 Mbaud, $\alpha = 0.2$	4 dB	9.02 dB
256APSK-L	2/3	17 Mbaud, $\alpha = 0.05$	15.5 dB	9.05 dB

Table 4.5: Simulation parameters for DSNG scenario

4.3.3 Performance evaluation

Also in this section the PER in function of P_{SAT}/N_0 will be evaluated, according to the definition of P_{SAT}/N_0 in 4.6. Afterward the related spectral efficiency will be calculated by mean of 4.7.

The generated signals are used as system input in Figure 4.22, and the sequence spectrum in downlink is the one shown in Figure 4.28.

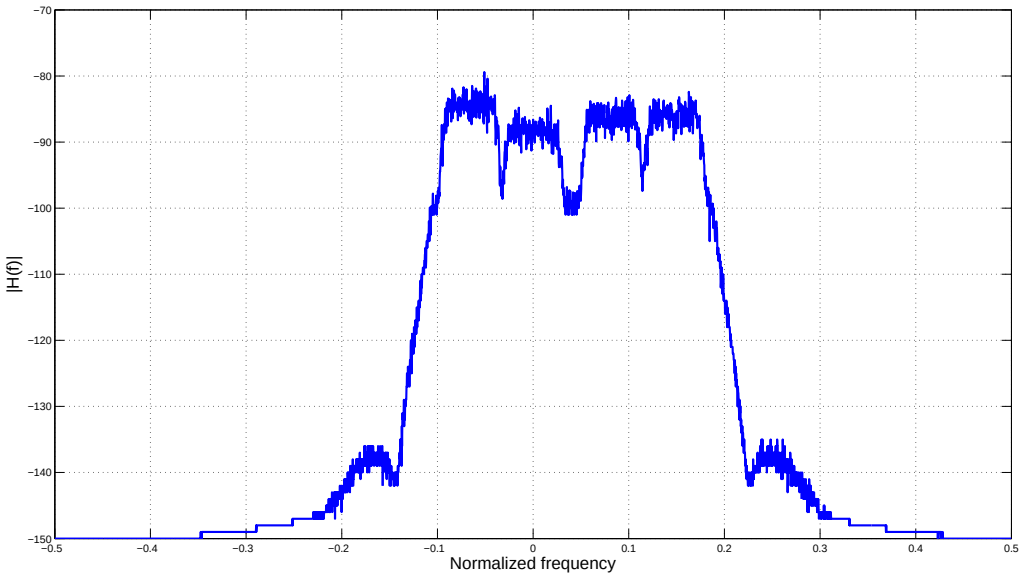

Figure 4.28: Normalized spectrum of the downlink sequence in DSNG scenario

The power normalization is implemented like in the previous cases, hence transmitted power equals to one with IBO/OBO equal to zero, and negative power (in dB) if the HPA is working in backoff.

Following the channel scheme in figure 4.22, thus with power unbalance $-4\,\mathrm{dB}$, the PER values in Figure 4.29 and 4.30 have been found out.

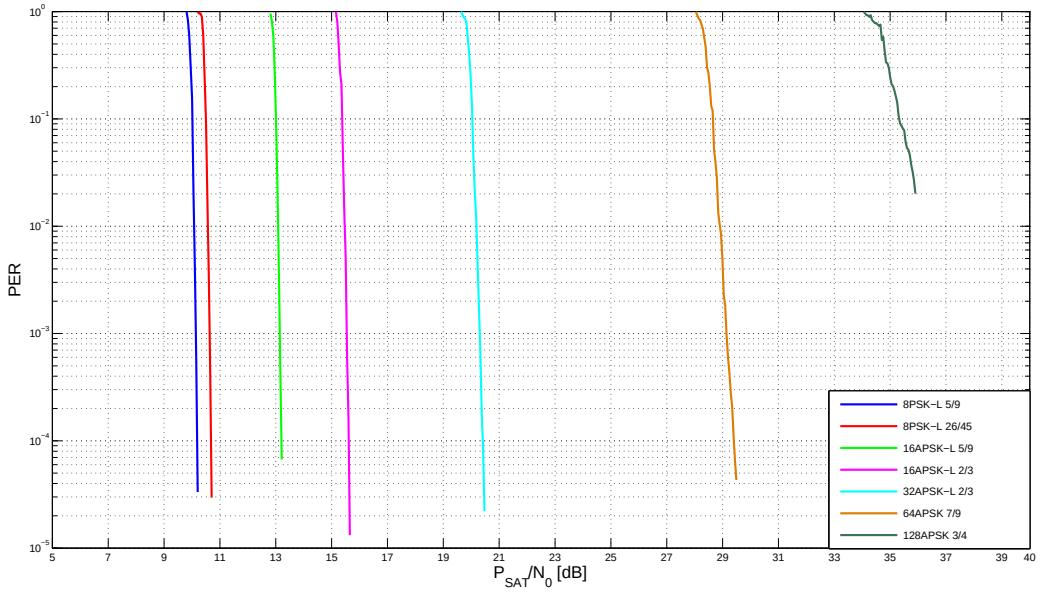

Figure 4.29: Packet Error Rate in DSNG scenario with $\alpha = 0.2$

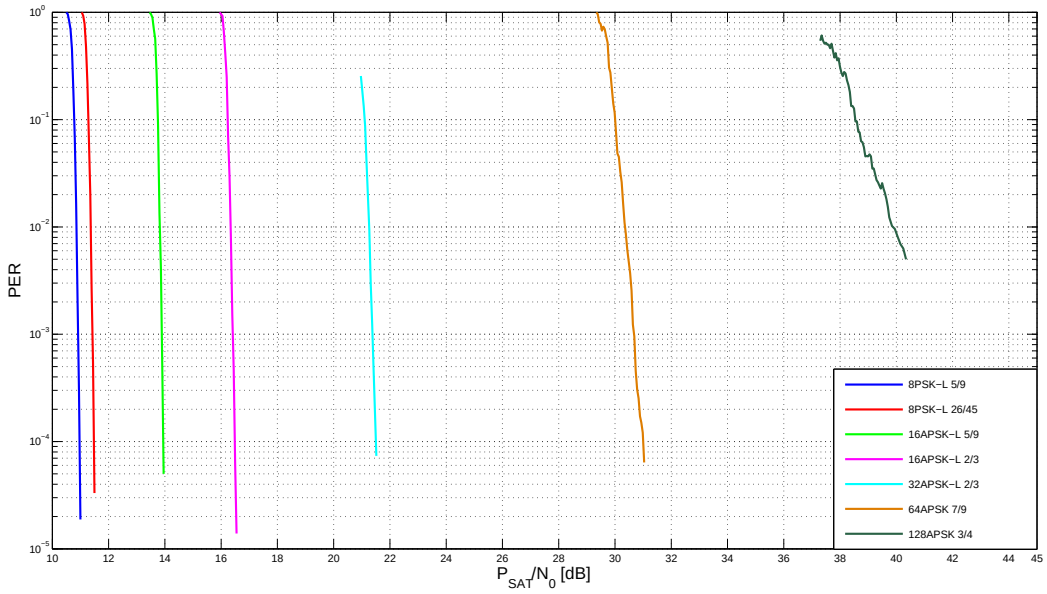

Figure 4.30: Packet Error Rate in DSNG scenario with $\alpha = 0.05$

The first thing that can be noticed is that one of the aforementioned modulations is missing in the outcomes: it is 256ASPK 3/4. This happened because, from the computer simulations results, it has been seen that this kind of MODCOD does not work in this scenario with power unbalance condition. As a matter of fact its PER does not have a real waterfall region, the error probability saturates at nearly 10^{-2}, the PER trend has not been plotted for sake of figure clearness. In order to have this MODCOD working we must be in favorable attenuation condition on the channel under test. However the evaluation of this modulation will not be neglected, since in Figure 4.31 the system performance without power unbalance have been examined.

Like in VSAT scenario the roll-off $\alpha = 0.2$ transmission setting is more efficient in terms of PER. However we achieve better spectral efficiency with $\alpha = 0.05$, this is due to the higher Baud Rate value.

Finally we would like to deepen the case with clear sky condition in uplink, in order to appreciate the degradation given by the attenuation. In Figure 4.31 PER curves are plotted for every MODCOD, using roll-off $\alpha = 0.05$. Of course, setting roll-off $\alpha = 0.2$, we reach similar results.

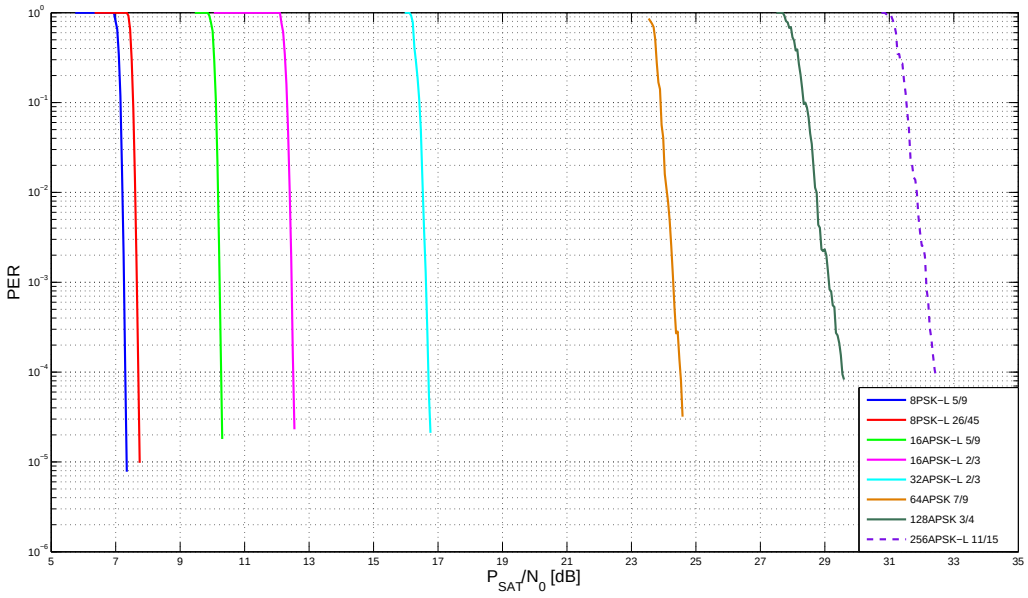

Figure 4.31: Packet Error Rate in DSNG scenario in clear sky condition with $\alpha = 0.05$

Since we evaluated the system performance without attenuation, it is possible to compare the two scenarios in order to quantify the losses given

by the uplink attenuation.

In Figures 4.32 and 4.33 both (with and without power unbalance) trends of PER are plotted for every MODCOD.

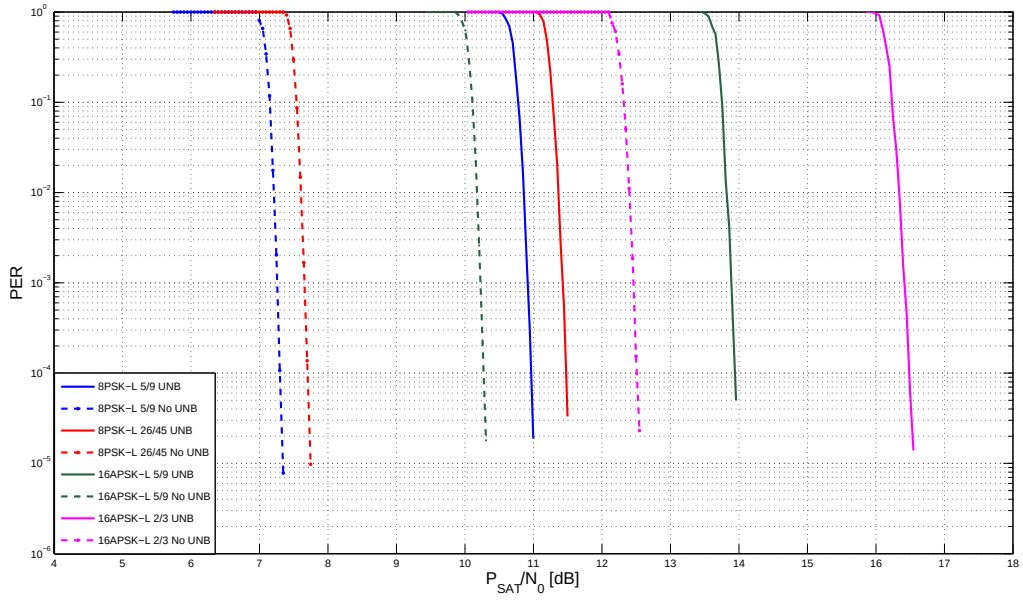

Figure 4.32: Comparison between Packet Error Rate in DSNG scenario in clear sky and power unbalance conditions with $\alpha = 0.05$. Lower order MODCODs

For lower order modulations the performance degradation is around 4 dB, which is close to the attenuation value. However the gap between power unbalance and clear sky condition increases with the order of the MODCOD. In Table 4.6 the gap values between the two scenario are expounded.

Modulation	Gap
8PSK-L 5/9	3.7 dB
8PSK-L 26/45	3.8 dB
16APSK-L 5/9	3.8 dB
16APSK-L 2/3	4 dB

Table 4.6: Gap between power unbalance scenario and clear sky one.(1)

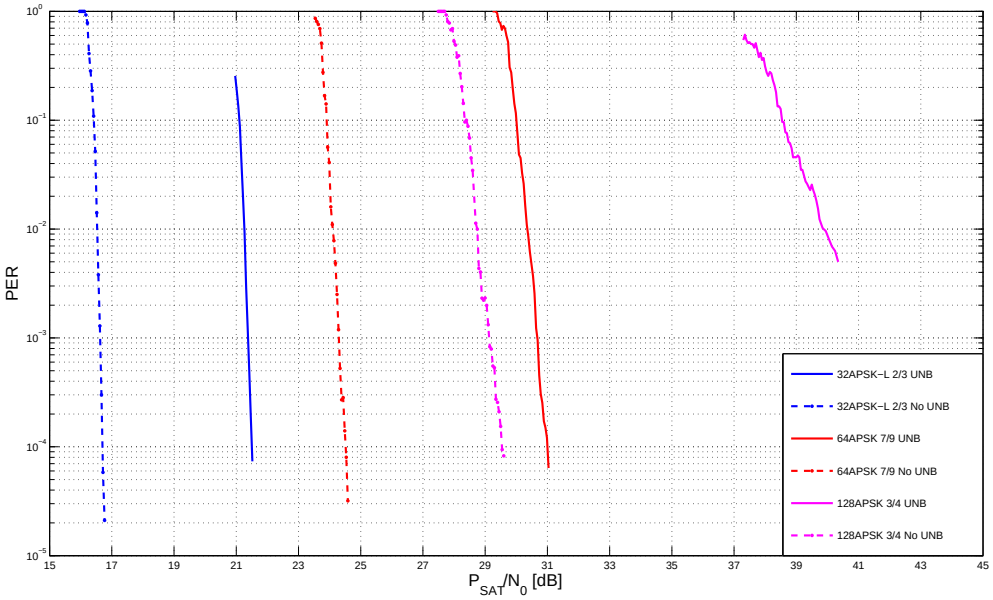

Figure 4.33: Comparison between Packet Error Rate in DSNG scenario in clear sky and power unbalance conditions with $\alpha = 0.05$. Higher order MODCODs

Setting the most efficient MODCODs, the gap between the two cases becomes dramatically huge, and the unbalanced scenario performance are much worse. This is due to the inter-modulation products and to the distortion given by the HPA, which, in case of high order constellations, are really strong impairments. Table 4.7 gives the gap values in the case of higher order modulations. 256APSK is not available in this because, as said before, in the power unbalance case it is not usable.

Modulation	Gap
32APSK-L 2/3	4.7 dB
64APSK 7/9	6.5 dB
128APSK 3/4	10.8 dB

Table 4.7: Gap between power unbalance scenario and clear sky one. Higher order modulations

Thus, from these last considerations, it is clear that power unbalance introduces some issues which are beyond the simple uplink power loss, espe-

cially for high order modulation, since the highest order MODCODs do not work or have waterfall region also for very high and very unlikely P_{SAT}/N_0 values.

Finally the power unbalance system spectral efficiency has been evaluated my mean of 4.7, and the outcomes are in Figure 4.34

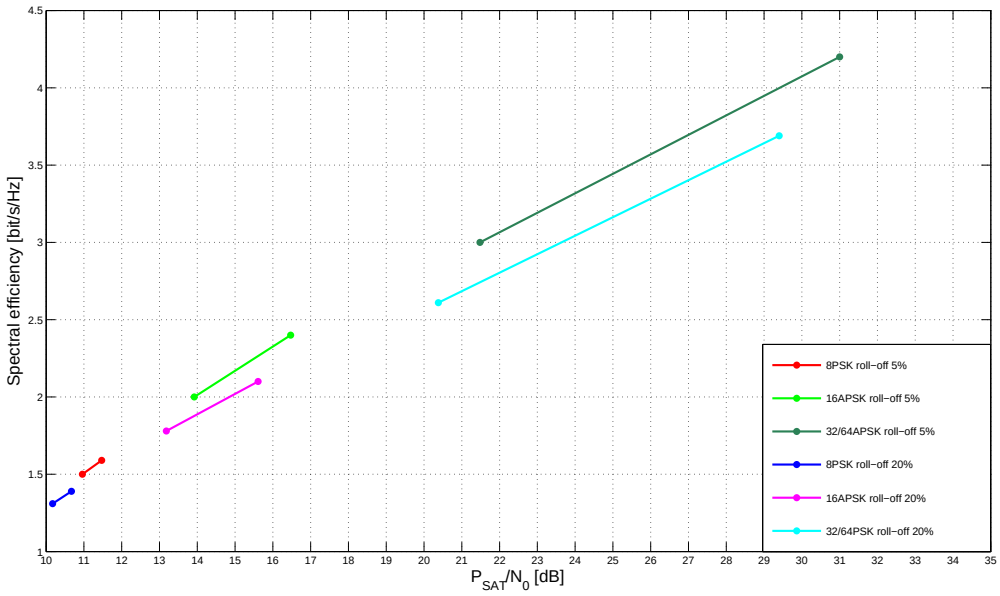

Figure 4.34: Spectral efficiency of DSNG scenario

Like in VSAT scenario $\alpha = 0.05$ setting is more efficient for its higher Baud Rate. The $\alpha = 0.2$ reaches the error threshold before, but this is not sufficient in order to outperform roll-off 5% symbol rate.

Chapter 5

Implementation of the simulator

This Chapter will go through a brief overview about the implementation of the simulator used for the performance evaluation of DVB-S2X MODCODs. The work has been carried out using TOPCOM library, which is a set of C++ classes developed by *Politecnico di Torino*, that implement plenty of algorithms for telecommunications from the regular modulations to OFDM and beyond. The main work was understanding, using and modifying these classes in order to create the block schemes analyzed in Chapter 4. The most important classes which have been used are *DVBS2X_ Transmitter*, *Transponder*, *AWGN_ Channel*, some classes about digital signal processing such as *Frequency_ Shift*, and finally, the most important one, *Satellite_ Channel*.

5.1 DVB-S2X transmitter and receiver

DVBSX_ Transmitter class implements all the DVB-S2X standard transmission settings. The transmission configuration is set using several functions, the most important are the following:

- *AddTXFilter* which, given the number of samples per symbol and the roll-off value, initializes a SRRC filter;
- *SetMODCOD* allows to choose the MODCOD under test, which is identified by an integer number;
- *TunePredistortion* applies to the transmitted sequence a pre-distortion technique; it requires three parameters which are the number of input samples, the pointer to the transponder, and the desired OBO value.

In order to modulate and encode the input sequence, *Run* method is available. It requires the pointers to the input sequence, to the output array, and the number of encoded frames.

In order to set up the receiver *DVBSX_ Receiver* class is available. Basically it requires a pointer to the *DVBSX_ Transmitter* object using *SetDetector* function, and afterward it can accomplish the decoding process with its *Run* function.

5.2 Transponder

Transponder class implements the satellite transponder block. It is composed of two main functions, like most of TOPCOM classes: *SetParameters* and *Run*. The first requires the pointers to the I/O-MUX filters and to the TWTA objects, the latter, which is responsible for the signal processing, the number of complex input samples and the pointer to the input and the output vectors.

In this work we used two *Transponder* friend classes, which are *DVBSX_ Transponder* and *DVBSX_ Transponder_ 500*. The operation is similar to the original class, since we exploit the *Run* function, but *SetParameters* is not necessary anymore, since it is intrinsic in the object initialization. The parameters required for the object generation are three boolean variables, that indicate if I/O-MUX filters and TWTA are simulated, an integer that specifies the type of non-linearity and finally the transponder 3 dB bandwidth.

5.3 AWGN channel

AWGN_ Channel class takes as input a noiseless sequence of samples, and gives as output noisy samples according to the set SNR and to the original stream. Therefore the output of *Run* method is given by

$$s[i] = x[i] + Pn[i] \tag{5.1}$$

where x is the input sequence, s the output, n a samples series of a Gaussian process with variance $\sigma^2 = 1$, and P sets the noise level since is expressed by

$$P = \sqrt{\frac{N_0}{2}} \tag{5.2}$$

In order to decide the SNR level *SetParameters* function is available, where the user specifies the SNR E_s/N_0 and the seed for the initialization of the Gaussian generator.

For the processing of a complex sequence it is sufficient to generate a double sized array, in which the even indexes elements are the real part, and odd indexes are the complex one.

5.4 Frequency shift

The class *Frequency_ Shift* has been crucial for the satellite channel models implementation, because in all of them different carriers have a precise position in frequency, thus, in order to make the system work properly, frequency shift had to be used correctly.

Basically the method *SetParameter* requires the normalized frequency shift value, which has to be expressed by mean of a ratio of two integers N and D. Hence, after we have set the integers N and D, *Run* function applies to the input sequence the following operations

$$Re\left(s\left[i\right]\right) = cos\left(2\pi\frac{N}{D}i\right) Re\left(x\left[i\right]\right) - sin\left(2\pi\frac{N}{D}i\right) Im\left(x\left[i\right]\right) \tag{5.3}$$

$$Im\left(s\left[i\right]\right) = cos\left(2\pi\frac{N}{D}i\right) Im\left(x\left[i\right]\right) + sin\left(2\pi\frac{N}{D}i\right) Re\left(x\left[i\right]\right) \tag{5.4}$$

We must remind that N/D is equal to the ratio f/T_s, where f is the actual value of the frequency shift and T_s is the sampling period.

5.5 Satellite channel

Satellite_ Channel class is the main component of the simulation chain. It is based on three groups of functions correspondent to the different channel schemes presented in Chapter 4.

The functions used for DTH channel simulations are *SetParameters_ DTH* and *Run_ DTH*. The first one is responsible for the parameters setting of the channel such as carrier baud rate, transponder bandwidth, number of samples per symbol, uplink attenuation value, carrier phase noise mask and receiver distortion. Therefore the function initializes all the desired channel components according to DTH settings described in Section 4.1, thus it creates and sets the parameters of *Delay*, *ShiftFrequency*, *Transponder* and *Phase_ Jitter* objects. *Run_ DTH* instead processes the input sequence correspondingly to *SetParameters_ DTH* information and to DTH channel scheme.

The crucial steps of the processing are the following:

- given an input sequence *Delay* and *ShiftFrequency Run* functions are applied in order to obtain the scheme in Figure 4.2 and all the resulting arrays are summed up in an *output* vector;
- next step is filtering *output* vector using *Transponder Run* function;
- finally interference in downlink is implemented in a similar manner of the uplink one, and phase noise and amplitude distortion are run as well.

As far as VSAT channel is concerned, *SetParameters_ VSAT* and *Run_ VSAT* functions are available. The functions structure is really similar to DTH one, but there are some differences due to the different channel scheme. For instance *SetParameters_ VSAT* requires two different transponder initializations due to the presence of the Diplexer, one of them is built without OMUX filter, the other instead degenerates in a simple OMUX. The reason for this kind of implementation is that 500 MHz satellite transponder has a different bandwidth with respect to the Diplexer, which, since it divides the two transmission beams, has only half bandwidth available.

Next *Run_ VSAT* processing function was implemented. It follows a similar procedure to the DTH version:

- allocates on an vector *output* the sum of the shifted and delayed input versions, accordingly to the channel model;
- on the satellite segment the diplexer implementation is based on two consecutive transponders; the first in the chain acts as IMUX and HPA, then the beam under test is temporarily shifted in baseband in order to be filtered by the OMUX;
- the downlink segment provides the translation of the OMUX output at the original frequency, the generation of the interferent beam, the application of the phase-noise and amplitude distortion.

All the listed procedures are accomplished by means of the same functions used in DTH version.

Finally *SetParameters_ DSNG* and *Run_ DSNG* are developed similarly to the aforementioned functions. The variations of *SetParameters_ DSNG* respect to the others are the initialization of two equal transponders, due to the DSNG scheme, and the frequency plan, which is really different.

Run_ DSNG function proceeds accordingly to channel scheme:

- it processes the input sequence by means of frequency shifts and delays, and allocates two arrays signal;
- transponder segment provides the amplification of these sequence independently;
- in downlink section, using delays and frequency shifts, the overall multicarrier signal is constructed summing the two arrays, outputs of the transponder section;
- the final part of the chain is identical to the previous cases.

Satellite_Channel is fully flexible, and in the next Section we will examine how it is introduced in the main loop.

5.6 Main simulation loop

In this last section we will examine the most important features of the main simulation loop. The routine reads the variables from a *txt* input file, and the required parameters are the following:

- maximum number of evaluated frames, and the maximum number of counted frames in error;
- the SNR gap from the AWGN QEF threshold;
- the MODCOD under test;
- indication of the presence of pre-distortion, and in affirmative case the OBO target, if not the IBO value;
- all the required parameters of *Satellite_Channel* class;
- the roll-off value;
- the channel type.

The first step is initializing and setting the transmitter parameters (e.g. SRRC filter, MODCOD). Afterward the *Satellite_Channel* object is initialized and a *SetParameters* function is called accordingly to the type of channel chosen in the input file. Finally the receiver is set pointing on the object which identifies the transmitter.

The main loop sequence proceeds according to the following steps, which are only the most important since the whole program accomplishes more operations than the listed ones:

- it generates a PN sequence;
- the sequence is processed by *DVBSX_ Transmitter Run* procedure, in order to build the modulated and encoded signal;
- the complex signal is processed by one of the *Run* functions defined in *Satellite_ Channel*, accordingly to the channel choice;
- AWGN noise is added to the sequence under test;
- finally the noisy signal is processed by *DVBSX_ Receiver Run* function;
- the last step of the loop is evaluating the PER.

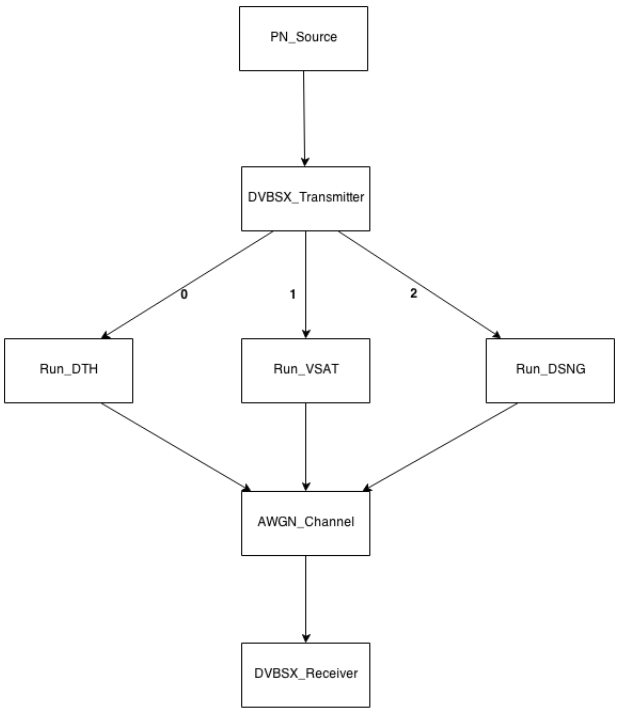

Figure 5.1: Simulator simplified implementation scheme

Figure 5.1 shows the simplified implementation scheme. It can be noticed that the procedure is similar for all channel models, the only difference is about the *Satellite_ Channel* function used, which is chosen on the input file with an interger number: 0 is associated with the DTH channel, 1 with VSAT and finally 2 with DSNG.

Chapter 6

Conclusion and final considerations

In this thesis a brief overview of DVB-S2X has been carried out, and it was possible to appreciate all the potential that this extension has. As a matter of fact it will open new paths in the SATCOM environment and spread new technologies, like, as we said in Chapter 1, new television standards such as UHDTV or 3DTV, and high-speed internet links as well. The system spectral efficiency has been improved thanks to new modulations available such as 64APSK, 128APSK and 256APSK, which were not present in DVB-S2, and to the code rates available.

In Chapter 3 the most common satellite environment impairments were explained. In particular we characterized the satellite transponder, composed by IMUX, OMUX and TWTA, which introduces both linear and non-linear distortion on the constellation. Afterward an analysis of the other components of the satellite channel such as interference, phase noise and cable distortion has been accomplished.

Finally three different transmission scenarios were presented which are DTH, VSAT and DSNG, and the performance of DVB-S2X over such schemes were evaluated with different MODCODs and transmission settings. From the simulation results we found out that in terms of PER setting roll-off %20 on the SRRC filter is always convenient, but in terms of spectral efficiency the situation changes. As a matter of fact in a single carrier scenario like DTH, MODCODs spectral efficiency evaluated with roll-off $\alpha = 0.2$ is always higher with respect to the ones using $\alpha = 0.05$, this happens because, since the transponder amplifies only one signal, the bandwidth allocation can be the equal for both roll-off values. Conversely on a multi-carrier scenario, MODCODs using roll-off $\alpha = 0.05$ are more efficient, this is due to their higher bandwidth, because with more than one signal per transponder we

cannot allocate the same bandwidth for both roll-off values, thus carriers with roll-off $\alpha = 0.2$ even though they perform better in terms of errors, since they have less bandwidth available, are less efficient.

One topic which can be further deepen is the degradation due to the attenuation in a multi-carrier mode. In fact in this work we only showed the degradation values for every MODCOD, but we did not characterized in a precise manner the performance loss brought by this impairment. Hence this topic could deserve an in depth analysis.

Finally DVB-S2X is a quite new extension of the older DVB-S2, therefore all its potentialities and its applications are yet to be explored, but it will be really useful for great improvements on the SATCOM field.

Appendix A

Frequency estimation

In this appendix we will evaluate the degradation, in terms of frequency error, introduced by the satellite transponder. Two different algorithms will be examined, which are the Maximum Likelihood (also known as Rife & Boorstyn algorithm) and Luise-Reggianini, and the performance in AWGN channel and basic satellite channel will be compared.

Maximum Likelihood algorithm

Defining $x(k)$ the received signal, we extract the input sequence for the estimation algorithm. Like [20] suggests the input sequence is given by A.1 in data aided case

$$z(k) = x(k)\, c^*(k) \tag{A.1}$$

and by equation A.2 in the case of non-data aided mode

$$z(k) = e^{jMarg[x(k)]} \tag{A.2}$$

where $x(k)$ is the received sample, and $c(k)$ is the sent one.

The algorithm presented in [21] basically consists in finding the maximum of the Fast Fourier Transform (FFT) of the input sequence $z(k)$. So we remind that the input FFT is given by espession A.3

$$Z(f) = \frac{1}{L_0} \sum_{k=0}^{L_0-1} z(k)\, e^{-j2\pi kfT} \tag{A.3}$$

where L_0 is the observation length, and it is a parameter of the algorithm.

Formally, the estimator output is given by equation A.4

$$\hat{f}_d = arg\left[max\left|Z(f)\right|\right] \tag{A.4}$$

The maximum search can be achieved in two steps. The coarse search which finds a maximum over a discrete set of f values, and the fine search which interpolates the result by a factor N, which is a parameter of the algorithm as well, and computes the local maximum closest to the outcome of the coarse search.

In Figures A.1 and A.2 the estimation variance is examined in both AWGN and satellite scenario. In AWGN scenario the estimator converges to the Cramer Rao bound, instead the transponder introduces a degradation in the performance, because the variance of the error is slightly higher in every SNR point, and saturates in a value close to 10^{-10} for high SNR values.

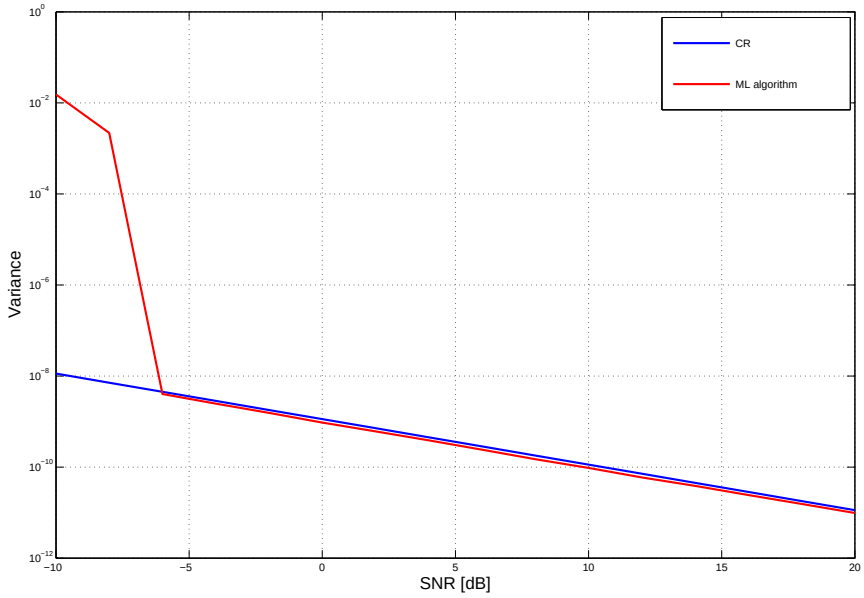

Figure A.1: Error variance of ML algorithm on AWGN channel

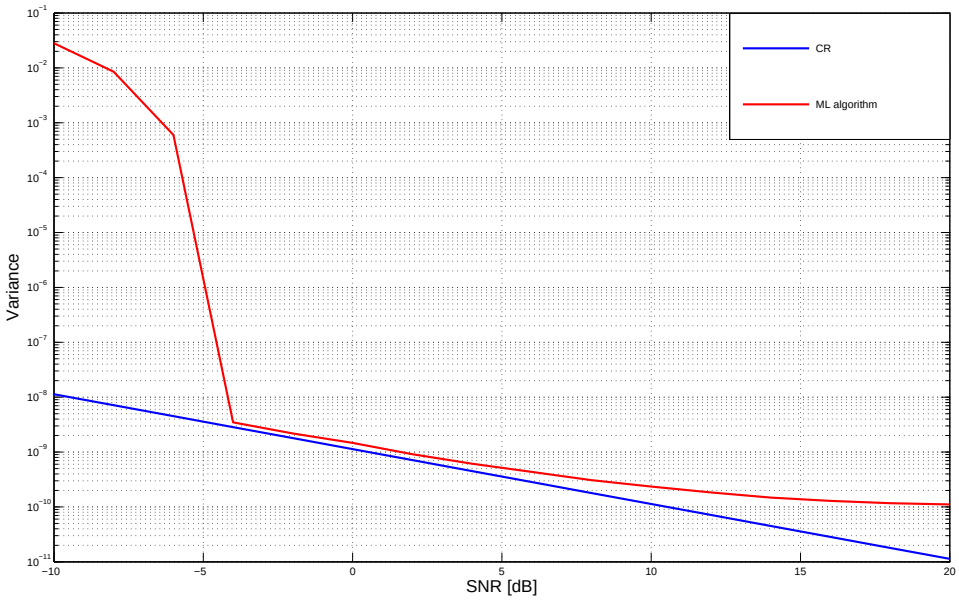

Figure A.2: Error variance of ML algorithm on satellite channel

Both simulations are carried out setting $L_0 = 512$ samples.

Luise-Reggianini algorithm

Luise-Reggianini algorithm, which is presented in [22], exploits the correlation of the input sequence built by mean of Equation A.2 or A.1, depending on the non-data aided or data-aided version. Setting L_0 as a parameter, it calculates the correlation of the sequence on L_0 samples, which is the one in Equation A.5

$$R(m) = \frac{1}{L_0 - m} \sum_{k=m}^{L_0-1} z(k)\, z^*(k-m) \tag{A.5}$$

Then it is necessary to set a new parameter N, called lag of the Luise-Reggianini algorithm, which defines on how many correlation samples we sum in equation A.6, in order to find the carrier frequency offset of the received signal

$$\hat{f}_d = \frac{1}{\pi MT\,(N+1)} arg\left[\sum_{m=1}^{N} R(m)\right] \tag{A.6}$$

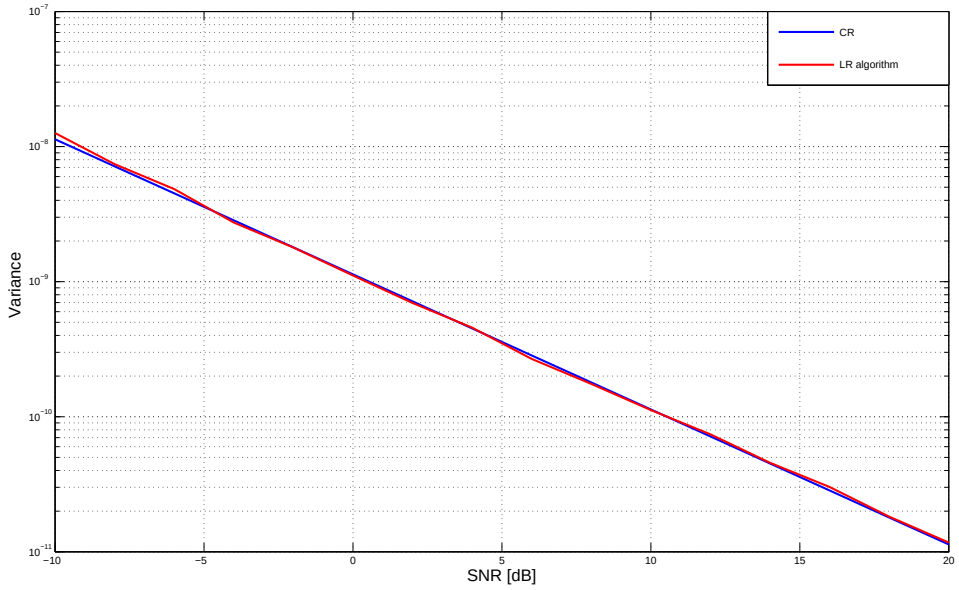

Figure A.3: Error variance of LR algorithm on AWGN channel

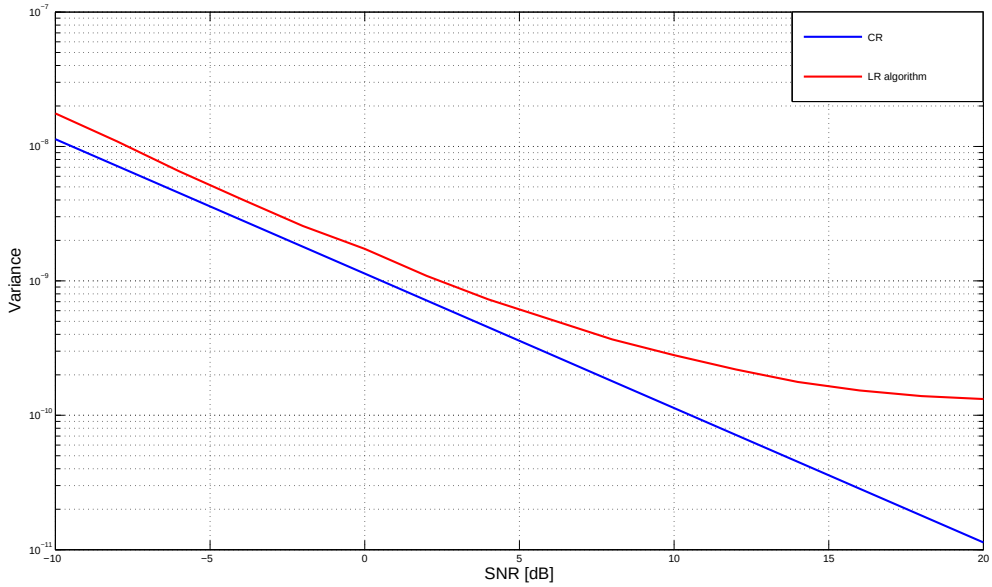

Figure A.4: Error variance of LR algorithm on satellite channel

The transponder effect, as can be seen in Figures A.3 and A.4, is quite

similar to one experienced with the Maximum Likelihood algorithm, since the variance of the estimation error in the AWGN case is strictly convergent to Cramer Rao bound, contrarily in the satellite channel introduces a light overall degradation and a variance saturation on 10^{-10} for high SNR values.

The parameters of the Luise-Reggianini algorithm were set accordingly to the ML case, therefore $L_0 = 512$ and $N = 256$.

Appendix B

MODCODs performance in AWGN channel

In this appendix we will show the QEF thresholds for all the simulated MODCODs, which are taken from [9] and [11]. In table B.1 all the SNR values regarding the DVB-S2 MODCODs are reported.

MODCOD	E_b/N_0 needed for QEF threshold
QPSK 1/4	$-2.35\,\mathrm{dB}$
QPSK 1/2	$1\,\mathrm{dB}$
QPSK 3/4	4.03 dB
8PSK 3/5	5.5 dB
8PSK 3/4	7.91 dB
8PSK 5/6	9.35 dB
16APSK 2/3	8.97 dB
16APSK 3/4	10.21 dB
32APSK 4/5	11.03 dB

Table B.1: DVB-S2 MODCODs performance over AWGN channel

As far as the DVB-S2X MODCODs are concerned, table B.2 reports all the performance in AWGN channel of the simulated SX2 MODCODs.

MODCOD	E_b/N_0 needed for QEF threshold
QPSK 13/45	−1.60 dB
8PSK 25/36	7.93 dB
8PSK-L 5/9	5.95 dB
8PSK-L 26/45	6.35 dB
16APSK 26/45	9.17 dB
16APSK 77/90	14.00 dB
16APSK-L 2/3	11.06 dB
16APSK-L 5/9	9.35 dB
32APSK 32/45	14.50 dB
32APSK-L 2/3	13.81 dB
64APSK-L 32/45	17.7 dB
128APSK 3/4	21.43 dB
256APSK-L 11/15	23.80 dB

Table B.2: DVB-S2X MODCODs performance over AWGN channel

Bibliography

[1] W. L. Pritchard, "The history and future of commercial satellite communications," *Vol.22 no.3 IEEE Communications Magazine*, 1984.

[2] J. N. Pelton, "The start of commercial satellite communications," *IEEE Communications Magazine*, 2010.

[3] P. Siebert, "Dvb: Developing global television standards for today and tomorrow," *Technical Symposium at ITU Telecom World (ITU WT)*, 2011.

[4] L. H. Mohammed El-Hajjar, "A survey of digital television broadcast transmission techniques," *IEEE Communications survey & Tutorials, Vol. 15. NO. 4, Fourth quarter 2013*, 2013.

[5] T. S. Vittoria Mignone, Maria Angeles Vazquez-Castro, "The future of satellite tv: The wide range of applications of the dvb-s2 standard and perspectives," *Vol.99, No.11,November 2011/ Proceedings of the IEEE*, 2011.

[6] R. R. Stefano Cioni, Riccardo De Gaudenzi, "Adaptive coding and modulation for the forward link of broadband satellite networks," *Globecom*, 2003.

[7] C. M. Eric Alberty, Sophie Defever, R. R. Riccardo De Gaudenzi, Alberto Ginesi, and A. V. Gennaro Gallinaro, "Adaptive coding and modulation for the dvb-s2 standard interactive applications: Capacity assessment and key system issues," *IEEE Wireless Communications*, 2007.

[8] K. Willems, "Dvb-s2x demystified," *Technical report, Newtec*, 2014.

[9] D. V. B. Group, "Etsi en 302 307, second generation framing structure, channel coding and modulation systems for broadcasting, interactive services, news gathering and other broadband satellite applications (dvb-s2)," *European Telecommunications Standard Institute*, 2005.

[10] D. V. B. group, "Etsi tr 102 376, user guidelines for the second generation system for broadcasting, interactive services, news gathering and other broadband satellite applications (dvb-s2)," *European Telecommunications Standard Institute*, 2005.

[11] D. V. B. group, "Etsi en 302 307, second generation framing structure, channel coding and modulation systems for broadcasting, interactive services, news gathering and other broadband satellite applications (part 2)," *European Telecommunications Standard Institute*, 2014.

[12] A. Morello and V. Mignone, "Dvb-s2: The second generation standard for satellite broad-band services," *Proceedings of the IEEE, Vol. 94, No.1*, 2006.

[13] G. Cherubini and N. Benvenuto, *Algorithms for Communications Systems and their Applications*. 2000.

[14] A. G. Enrico Casini, Riccardo De Gaudenzi, "Dvb-s2 modem algorithms desing and performance over typical satellite channels," *International journal of satellite communications and networking*, 2004.

[15] A. Ginesi, "Dvb-s2x channel models," 2014.

[16] M. A. Enrico Colzi, Piero Angeletti, S. D'Addio, R. O. Balague, and E. Casini, "Characterization of twta nonlinearity by means of a time-domain correlation method," 2008.

[17] G. Corazza, *Digital Satellite Communications*. 2007.

[18] S. C. Alberto Ginesi and M. Angelone, "Dvb-s2x channel models rationale and justifications," 2014.

[19] G. Maral and M. Bousquet, *Satellite communications systems*. 2009.

[20] M. Morelli and U. Mengali, "Feedforward frequency estimation for psk: a tutorial review," 1998.

[21] D. Rife and R. Boorstyn, "Single-tone parameter estimation from discrete-time observations," *IEEE transactions on information theory*, 1974.

[22] M. Luise and R. Reggianini, "Carrier frequency recovery in all-digital modems for burst-mode transmissions," *IEEE transactions on communications*, 1995.